

AD-A061 368

ROCKWELL INTERNATIONAL THOUSAND OAKS CALIF SCIENCE --ETC F/G 11/6  
DEFORMATION OF TEXTURED STEELS.(U)

SEP 78 A K GHOSH, N E PATON

DAAG46-77-C-0054

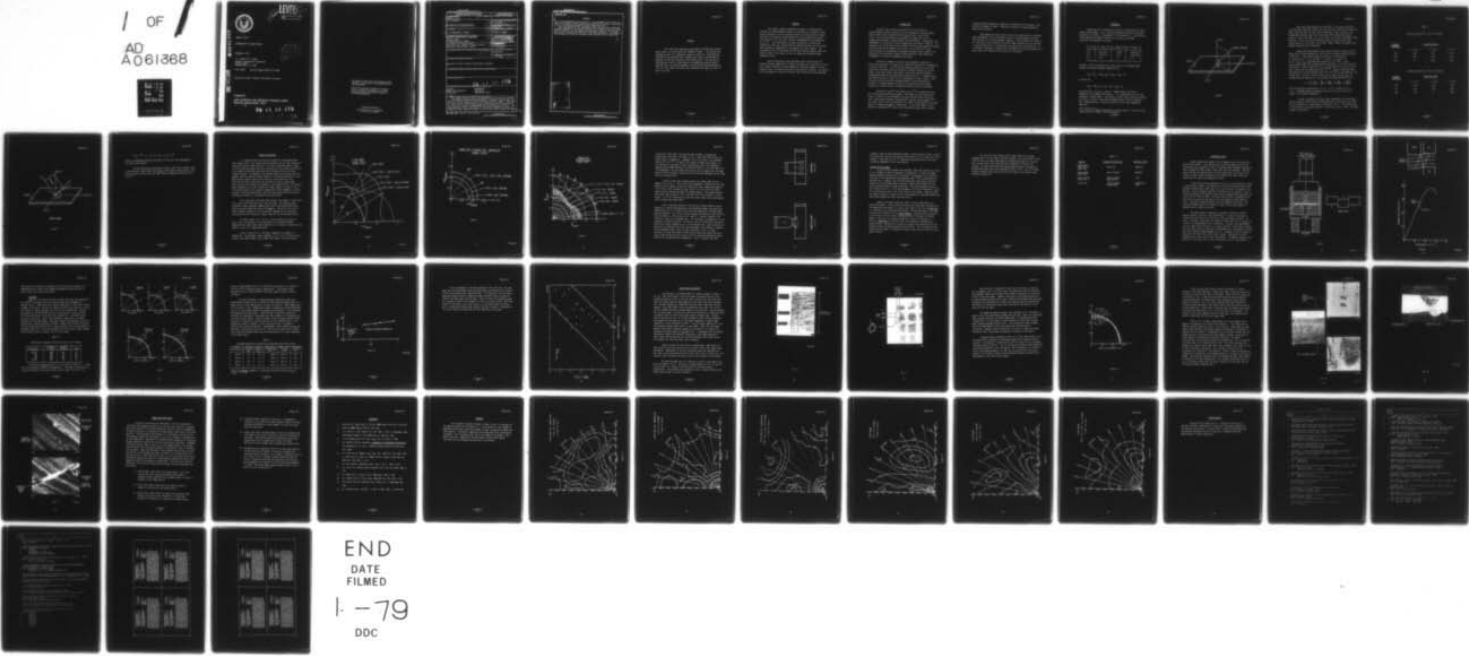
UNCLASSIFIED

SC5122.7FR

AMMRC-TR-78-40

NL

1 OF  
AD  
A061368



END  
DATE  
FILMED  
1-79  
DDC

OF

AD  
A061368



AD A061368

DDC FILE COPY



AAMRC TR 78-40

DEFORMATION OF TEXTURED STEELS

September, 1978

A. K. Ghosh & N. E. Paton

Rockwell International Corporation  
Science Center  
Thousand Oaks, CA 91360

Final Report      Contract Number DAAG-46-77-C-0054

Approved for public release; distribution unlimited.

Prepared for

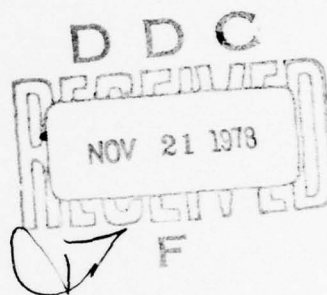
ARMY MATERIALS AND MECHANICS RESEARCH CENTER  
Watertown, Massachusetts 02172

78 11 15 174

78 11 15 154

12 LEVEL 3

AD



The findings in this report are not to be construed as an official Department of the Army position, unless so designated by other authorized documents.

Mention of any trade names or manufacturers in this report shall not be construed as advertising nor as an official indorsement or approval of such products or companies by the United States Government.

#### DISPOSITION INSTRUCTIONS

Destroy this report when it is no longer needed.  
Do not return it to the originator.



UNCLASSIFIED

SECURITY CLASSIFICATION OF THIS PAGE (When Data Entered)

REPORT DOCUMENTATION PAGE		READ INSTRUCTIONS BEFORE COMPLETING FORM
1. REPORT NUMBER AMMRC TR-78-40	2. GOVT ACCESSION NO.	3. RECIPIENT'S CATALOG NUMBER
4. TITLE (and Subtitle) Deformation of Textured Steels.	5. TYPE OF REPORT & PERIOD COVERED Final Report. 15 Aug 77-15	6. PERFORMING ORG. REPORT NUMBER SC5122.7 FR
7. AUTHOR(s) A. K. Ghosh & N. E. Paton	8. CONTRACT OR GRANT NUMBER(s) DAAG46-77-C-0054	9. PROGRAM ELEMENT, PROJECT, TASK AREA & WORK UNIT NUMBERS D/A Project IL162105AH84 AMCMS Code: 312105.H840011 Agency Accession: DA 0B4807
10. CONTROLLING OFFICE NAME AND ADDRESS Rockwell International Corporation Science Center Thousand Oaks, CA 91360	11. REPORT DATE September 1978	12. NUMBER OF PAGES 45
13. MONITORING AGENCY NAME & ADDRESS (if different from Controlling Office)	14. SECURITY CLASS. (of this report) Unclassified	15. DECLASSIFICATION/DOWNGRADING SCHEDULE N/A
16. DISTRIBUTION STATEMENT (of this Report)  Approved for public release; distribution unlimited.		
17. DISTRIBUTION STATEMENT (of the abstract entered in Block 20, if different from Report)		
18. SUPPLEMENTARY NOTES		
19. KEY WORDS (Continue on reverse side if necessary and identify by block number) Texture                      Deformation Preferred Orientation      Ballistics Alloy Steel                  Compression Tests		
20. ABSTRACT (Continue on reverse side if necessary and identify by block number) The present research program was designed to investigate the influence of crystallographic texture on the mechanical strength of steel plates subjected to various loading conditions including ballistic impact. The steels of interest are 5% Ni martenistic steels containing varying intensities of (111) and (112) textures, thermomechanically processed by Hu et al <sup>(1)</sup> . The investigation includes calculations of theoretical strength for shear and through thickness compression modes for the various ideal textures by computa-		

UNCLASSIFIED

SECURITY CLASSIFICATION OF THIS PAGE (When Data Entered)

389 949

Due

UNCLASSIFIED

SECURITY CLASSIFICATION OF THIS PAGE(When Data Entered)

Block No. 20

ABSTRACT

tion of the appropriate Taylor factors. The experimental part of the program involved shear testing samples taken from various angles in the plates, as well as conducting through-thickness compression tests.

Both the theoretical and experimental work indicate that the through-thickness compression resistance increases with increasing (111) and (112) texture intensity, and the compression resistance appears to be the dominant factor in controlling ballistic perforation resistance. An analysis of failure modes for plates of different ideal textures has also been made.

ACCESSION for	
NTIS	<input checked="" type="checkbox"/>
DDC	<input type="checkbox"/>
UNANNOUNCED	<input type="checkbox"/>
JUSTICIAL	
BY	
DISTRIBUTION	INDEXES
E	SPECIAL
A	

UNCLASSIFIED

SECURITY CLASSIFICATION OF THIS PAGE(When Data Entered)

FOREWORD

This report was prepared by the Rockwell International Science Center under U.S. Army Contract No. DAAG46-77-C-0054. The research was conducted as part of a cooperative program in which U.S. Steel Research Laboratories had developed high strength armor plates, the deformation mechanics of which was studied at the Science Center. The contract was administered by the U.S. Army Materials and Mechanics Research Center, Watertown, Ma., Mr. Anthone Zarkodes, Contracting Officer Representative. This is a final report and covers work conducted from August 15, 1977 to August 15, 1978.

ABSTRACT

The present research program was designed to investigate the influence of crystallographic texture on the mechanical strength of steel plates subjected to various loading conditions including ballistic impact. The steels of interest are 5% Ni martensitic steels containing varying intensities of (111) and (112) textures, thermomechanically processed by Hu et al<sup>(1)</sup>. The investigation includes calculations of theoretical strength for shear and through-thickness compression modes for the various ideal textures by computation of the appropriate Taylor factors. The experimental part of the program involved shear testing samples taken from various angles in the plates, as well as conducting through-thickness compression tests.

Both the theoretical and experimental work indicate that the through-thickness compression resistance increases with increasing (111) and (112) texture intensity, and the compression resistance appears to be the dominant factor in controlling ballistic perforation resistance. An analysis of failure modes for plates of different ideal textures has also been made.



## INTRODUCTION

Results from a recent investigation<sup>(1)</sup> on the effect of crystallographic texture on the ballistic performance of a medium-carbon 5Ni-Si-Cu-Mo-V steel indicated that the  $V_{50}$  ballistic limit of the (112) + (111) textured plates was substantially higher than that of random-textured plates at approximately the same hardness. Furthermore, the improvement in the ballistic limit increased with the texture intensity. The reproducibility of the results were further verified by more extensive studies on plates with various degrees of the (112) + (111) texture.<sup>(2)</sup> These studies opened up a new method of strengthening armor plates; however, the mechanism of such strength increase eluded explanation, even though the fundamentals of texture strengthening were known.

Preferred alignment of certain crystallographic directions in polycrystalline metals, is known to be a method of preferential strengthening in certain directions. The rolling and annealing practices of low carbon steels have long been controlled suitably to produce strong (111) texture normal to the sheet plane, which imparts significant through-thickness strengthening and excellent deep-drawing characteristics. It appeared that such effects might be related to the strengthening in armor plates. While the armor plates derive their strength primarily from the martensitic structure, it seemed appropriate that the calculation of texture-based strength for possible texture strengthening effects should be conducted.

The work of Taylor<sup>(3)</sup> and Bishop and Hill<sup>(4)</sup> are extensively used for calculating texture-based strength. The method for calculating Taylor factor,  $M$  (ratio of yield strength to critical resolved shear stress for slip), popularized by Hosford and Backofen<sup>(5)</sup> and Chin and co-workers,<sup>(6-8)</sup> for various ideal crystal orientations, has primarily been applied to uniaxial tension or compression modes of deformation. In ballistic impact, virtual absence of acceleration<sup>(9)</sup> gives rise to deformation modes that are either

through-thickness compression (identical to balanced biaxial tension in the plane of the sheet) or shear. Therefore, M factors for these deformation modes were calculated.

Even though the strain-rates for ballistic penetration are extremely high, deformation is still believed to occur by crystallographic slip and hence the need for a crystallographic approach. The calculation of M factors as a function of test direction for various ideal textures can also indicate if failure might occur in a shear mode or by petalling or back spalling. It is therefore, important to develop such information to guide the production of steel plates for a desired kind of ballistic resistance.

BACKGROUND

Bishop and Hill's procedure was used for calculating M for fixed imposed shape changes. Fig. 1 relates the impact direction to the sheet directions: rolling (r), transverse (t) and thickness (z). The direction cosines between the impact direction ( $a_1$ ,  $a_2$  and  $a_3$ ) and sheet directions are expressed as follows:

	$a_1$	$a_2$	$a_3$
$\underline{t}$	$\cos\theta \sin\alpha$	$-\sin\theta$	$-\cos\theta \cos\alpha$
$\underline{r}$	$\sin\theta \sin\alpha$	$\cos\theta$	$-\sin\theta \cos\alpha$
$\underline{z}$	$\cos\alpha$	0	$\sin\alpha$

Writing 1, 2 and 3 in places of  $a_1$ , and  $a_2$  and  $a_3$ , the imposed shape changes for through thickness compression are

$$d\epsilon_3 = 2d\epsilon_1 = -2d\epsilon_2; d\epsilon_{12} = d\epsilon_{23} = d\epsilon_{31} = 0;$$

and shear are

$$d\gamma_{21} = d\gamma_{31}; d\epsilon_1 = d\epsilon_2 = d\epsilon_3 = d\gamma_{23} = 0,$$

noting that  $\gamma_{21} = 2\epsilon_{21}$  etc., where  $\gamma$  = imposed shear strain and  $\epsilon$  = component of the imposed strain tensor. It is noteworthy that this shear represents a square shear.\* Calculation of planar shear involves assigning only  $d\gamma_{21} \neq 0$ , while a rotationally symmetric shear involves assigning  $d\gamma_{21} = d\gamma \cos\phi$  and  $d\gamma_{31} = d\gamma \sin\phi$  ( $0 \leq \phi \leq \frac{\pi}{2}$ ) with all other components being zero.

---

\*It is similar to shearing through with a square punch in 1 direction with shear strains on planes 2 and 3 being equal.



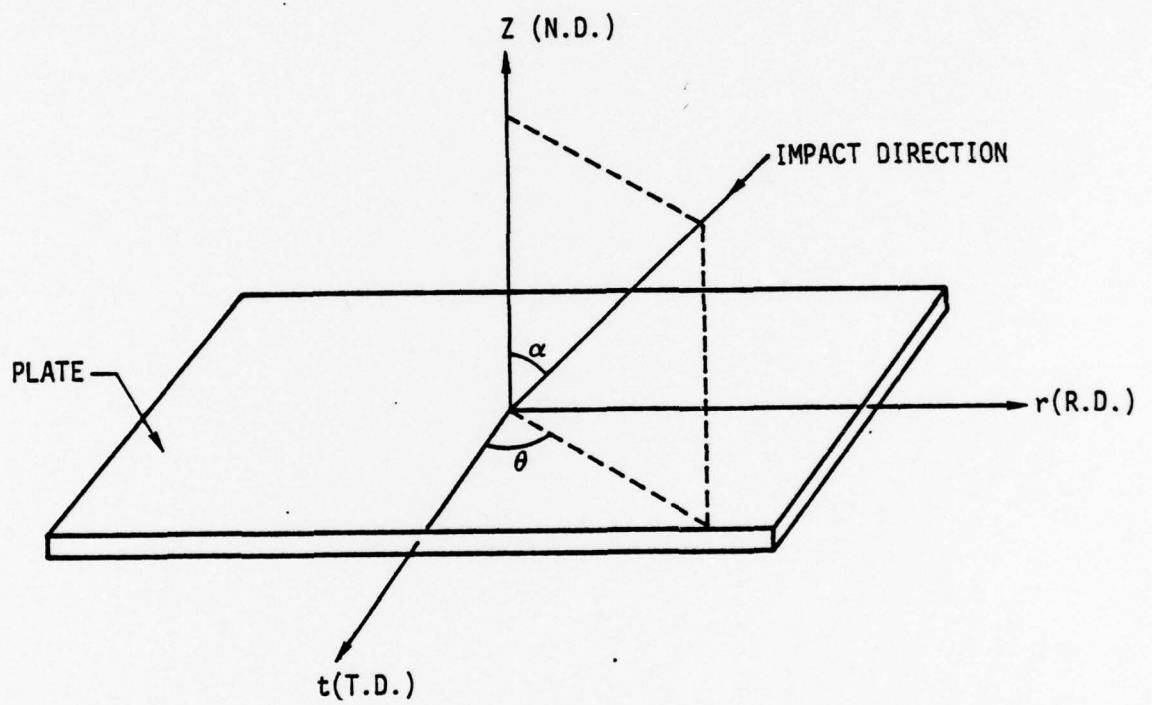


Figure 1

After these shape changes are resolved<sup>(4)</sup> in the sheet directions using the above direction cosines, they are resolved in the crystal directions (100), (010) and (001) for each ideal orientation. These are some of the orientations that were used by Hu and co-workers<sup>(1)</sup> to describe the pole figures of their 5-Ni steel, e.g. (111) <112>, (112) <110>, (110) <001>, (100) <023> etc. Table I lists the direction cosines for some of these ideal orientations e.g. (111) <112>, (112) <110>. Some of these also happen to be commonly observed ideal orientations.

Knowing the shape change in the crystal direction allows us to use Bishop and Hill stress-states for (110) <111> slip system for maximizing the virtual work. These stress-states are given by  $A = (\sigma_2 - \sigma_3) / \sqrt{6} \tau_s$ ,  $B = (\sigma_3 - \sigma_1) / \sqrt{6} \tau_s$ ,  $C = (\sigma_1 - \sigma_2) / \sqrt{6} \tau_s$ ,  $F = \sigma_{23} / \sqrt{6} \tau_s$ ,  $G = \sigma_{31} / \sqrt{6} \tau_s$  and  $H = \sigma_{12} / \sqrt{6} \tau_s$ , which can take values of 0,  $\pm 1/2$  and  $\pm 1$ , the stresses being taken with reference to the cube axes,  $\tau_s$  = critical resolved shear stress. Stress states for (112) <111> and (123) <111> slip as well as pencil glide have also been worked out,<sup>(7,10,11)</sup> however, these are rather inconvenient to use and therefore only (110) <111> slip is considered for the present work.  $M$ , which is given by  $dW / \tau_s d\gamma$  for shear and  $dW / \tau_s d\epsilon_3$  for through-thickness compression is obtained by finding the maximum value of

$$M = \sqrt{6} \left[ -B \frac{d\epsilon_1}{d\epsilon} + A \frac{d\epsilon_2}{d\epsilon} + 2F \frac{d\epsilon_{23}}{d\epsilon} + 2G \frac{d\epsilon_{31}}{d\epsilon} + 2H \frac{d\epsilon_{12}}{d\epsilon} \right]$$

from the 28 possible combinations of A, B.....H ( $d\epsilon$  stands for  $d\gamma$  or  $d\epsilon_3$ ). A FORTRAN computer program was written to do this work and the results are discussed subsequently.

In order to compare with planar shear experiments to be described in the next section, Taylor factors calculations were carried out by the Bishop and Hill method<sup>1</sup> for a shape change illustrated in Fig. 2. The planar shear is chosen here to be acting along the Z' direction on the X' plane. The shape change is described by

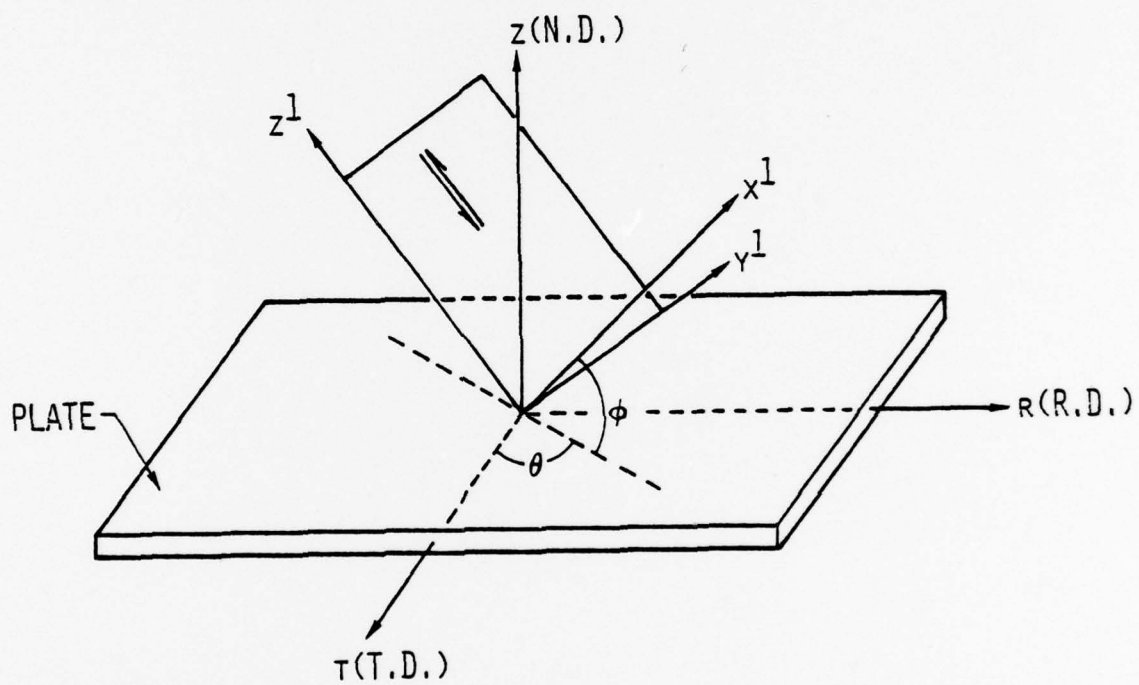
TABLE I

## Direction Cosines For (111) &lt;112&gt; Texture

<u>Crystal Directions</u>	<u>Sheet Directions</u>		
	$t = \langle 110 \rangle$	$r = \langle 112 \rangle$	$z = \langle 111 \rangle$
100	$1/\sqrt{2}$	$1/\sqrt{6}$	$1/\sqrt{3}$
010	$-1/\sqrt{2}$	$1/\sqrt{6}$	$1/\sqrt{3}$
001	0	$-2/\sqrt{6}$	$1/\sqrt{3}$

## Direction Cosines For (112) &lt;110&gt; Texture

<u>Crystal Directions</u>	<u>Sheet Directions</u>		
	$t = \langle 111 \rangle$	$r = \langle 110 \rangle$	$z = \langle 112 \rangle$
100	$-1/\sqrt{3}$	$1/\sqrt{2}$	$1/\sqrt{6}$
010	$-1/\sqrt{3}$	$-1/\sqrt{2}$	$1/\sqrt{6}$
001	$1/\sqrt{3}$	0	$2/\sqrt{6}$



PLANAR SHEAR

Figure 2

$$\gamma_{x'z'} \neq 0; \quad \epsilon_x = \epsilon_y = \epsilon_z = \gamma_{x'y'} = \gamma_{y'z'} = 0,$$

which is transformed along the cube axes of the crystal, and subsequently utilized in the analysis.

The calculations are performed for several ideal cubic textures, such as cube-on-face, (100) <001>, cube-on-edge, (110) <001>, cube-on-corner, (111) <112>; as well as (112) <110> and (100) <023> as prompted by the work of Hu et al.<sup>(1)</sup>



### RESULTS OF ANALYSIS

It is observed that the (110) pole figure for the quenched armor steel plate in Ref. 1 has strong intensity maxima on the rolling direction at nearly  $30^\circ$  from the normal direction. This pole figure described in terms of (111) planes thus means that only two particular (111) planes are parallel to the sheet surface whose adjoining (110) directions give rise to the intensity maxima. The absence of such maxima along the transverse direction, however, does not mean that shears normal to the transverse direction is any more difficult than in the rolling direction, since three  $\langle 112 \rangle$  slip directions at  $120^\circ$  to each other are available on each of these planes. Equal availability of these slip systems is thus responsible for the isotropic shear strength of (111)  $\langle 112 \rangle$  texture for normal impact, as shown in Fig. 3. It has been found by trial and error method that for the symmetry of rolling textures, only two reverse planes, each with two reverse directions need be considered including all the possible calculated values.

M for (100)  $\langle 023 \rangle$  and (100)  $\langle 001 \rangle$  textures are highest in shear while (111)  $\langle 112 \rangle$ , (110)  $\langle 001 \rangle$  and (112)  $\langle 110 \rangle$  are lower. Only cube-on-corner orientation shows rotational symmetry about the rolling plane normal while cube-on-face and (100)  $\langle 023 \rangle$  have a  $45^\circ$  symmetry. The (112)  $\langle 110 \rangle$  texture shows a greater strength in rolling direction compared to the transverse direction while this increase is rather large for the cube-on-edge texture.

For normal impact ( $\alpha = 0$  in Fig. 1) the M contours are shown in Figs. 4 and 5 as functions of in-plane angle  $\theta$ , for through-thickness compression and square shear modes respectively. M values are normalized with respect to that of a random polycrystal.

Figure 4 shows that all individual components are symmetric in compression. The strongest single component is (111)  $\langle 112 \rangle$  or cube-on-corner texture, being approximately 25% stronger than random. The cube-on-edge

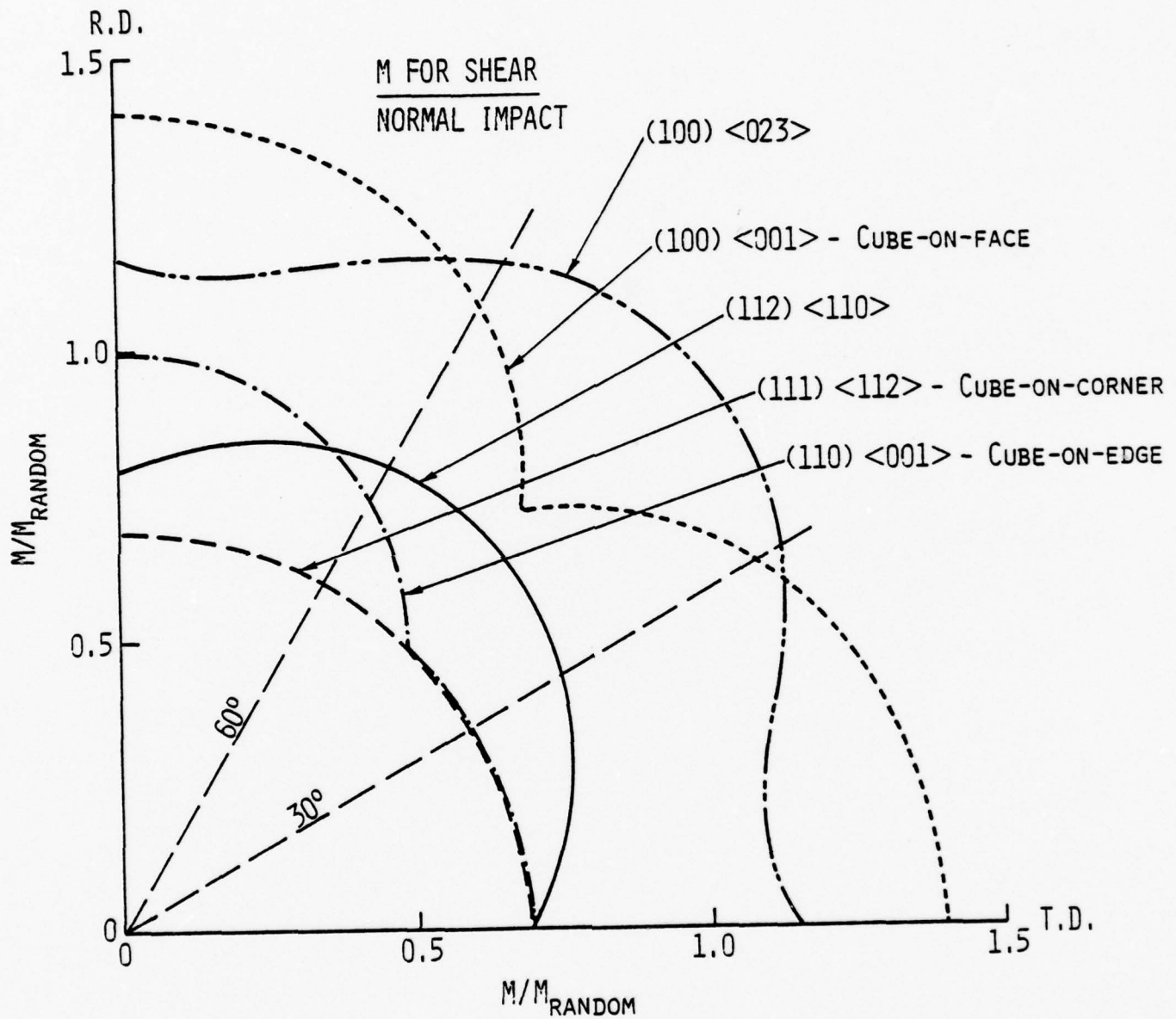


Figure 3



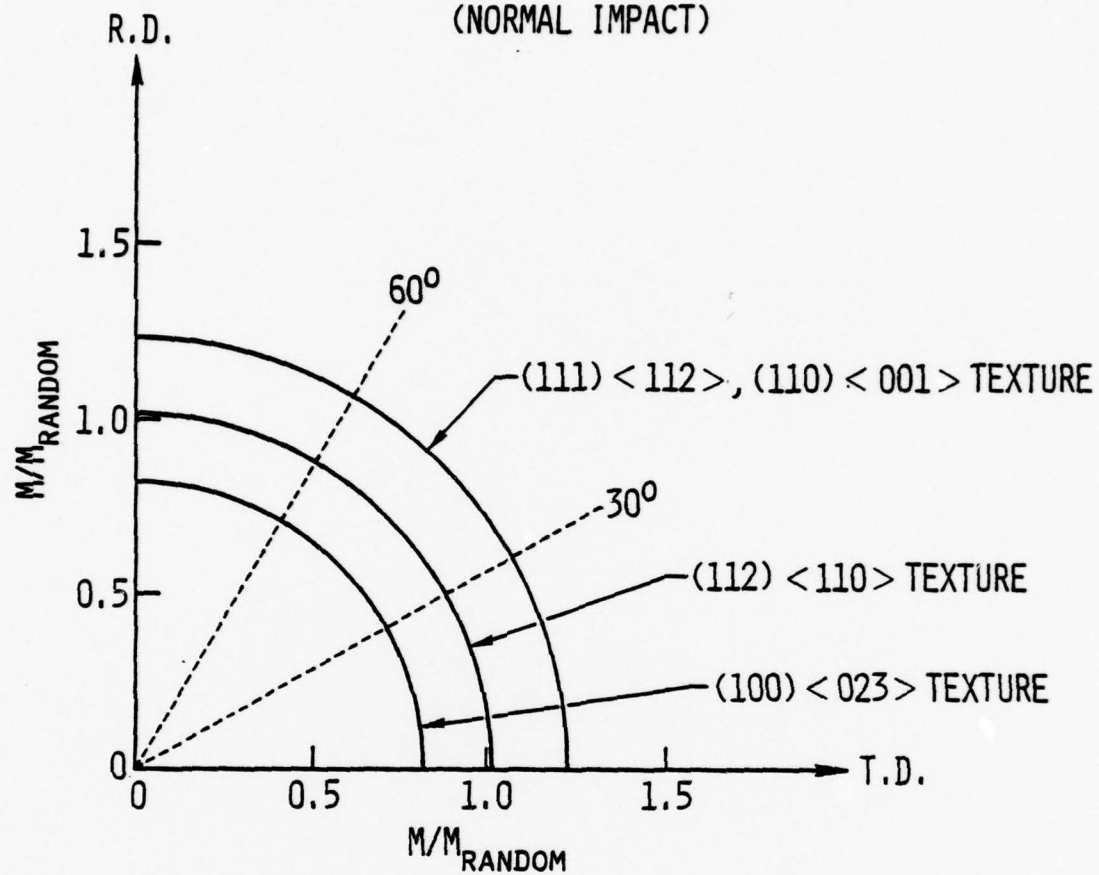
NORMALIZED M THROUGH THK. COMPRESSION  
(NORMAL IMPACT)

Figure 4

NORMALIZED M  
FOR SQUARE SHEAR  
(NORMAL IMPACT)

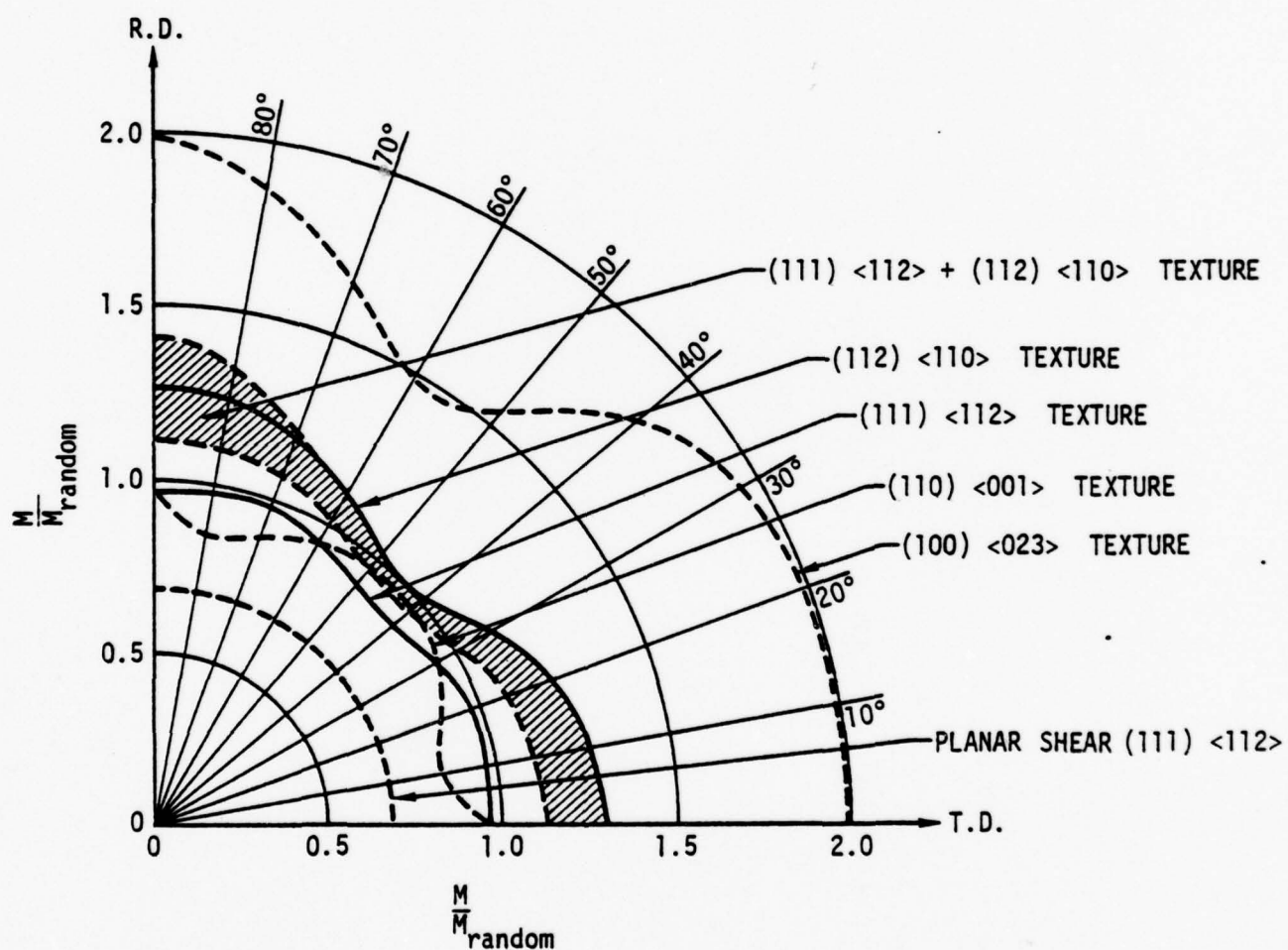
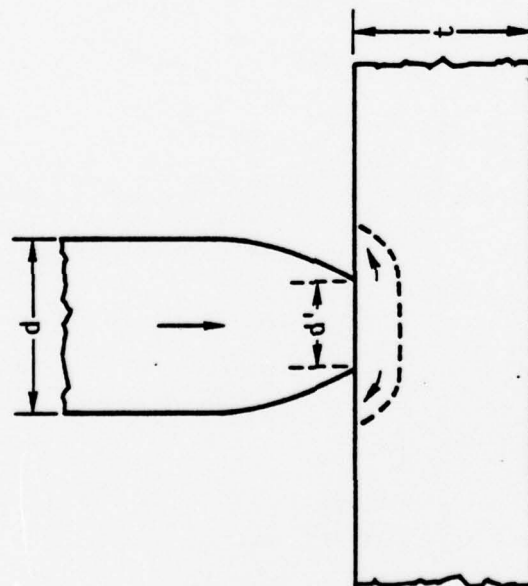


Figure 5

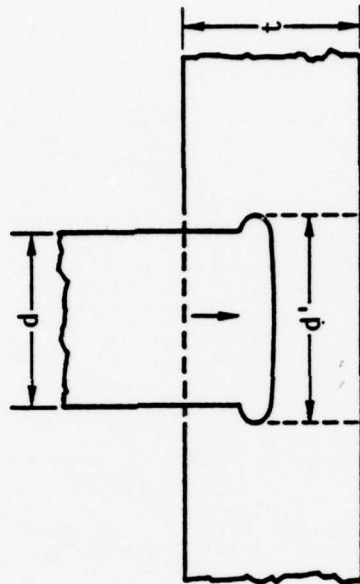
orientation  $((110) \langle 001 \rangle)$  also has the same strength in compression. Cube-on-face  $(100) \langle 001 \rangle$ , not shown in Fig. 2, and  $(100) \langle 023 \rangle$  texture are equally weak in compression. Component  $(112) \langle 110 \rangle$  found in the quenched plates of Hu et al.<sup>(1)</sup> is found to be slightly stronger than random. All real textures are mixtures of ideal orientations, and if one represents quenched steels (90% reduction) as mixtures of 50%  $(111) \langle 112 \rangle$  and 50%  $(112) \langle 110 \rangle$  components, one can expect  $M$  to be given by the shaded area, the upper bound of which is based on averaging slip for the two components and the lower bound for average stress.

Figure 5 shows that strength contours for square shear are not symmetric as in Fig. 3. Out of the single components, cube-on-face and  $(100) \langle 023 \rangle$  are the strongest, directly in contrast to their compression behavior.  $(112) \langle 110 \rangle$  is fairly strong in shear, while  $(111) \langle 112 \rangle$  and  $(110) \langle 001 \rangle$  (cube-on-corner and cube-on-edge) are somewhat weaker. The shaded envelope shows again that mixture of  $(111) \langle 112 \rangle$  and  $(112) \langle 110 \rangle$  textures is fairly strong. It is also interesting to note that planar shear yields considerably lower strength than square shear.

While a detailed analysis of the ballistic impact mechanics may be needed for a clearer understanding of the deformation modes, the simplified representation of Fig. 6 might explain why both compression and shear modes might be important. For initial contact between the projectile and the plate, plate thickness,  $t$ , being large ( $t \geq d'$ , where  $d'$  = contact diameter), the situation is much like a hardness test. The resistance to compression is thus important to prevent yielding. This may be true for 127 mm thick plate and a projectile of equal diameter ( $d$ ), as in the present case. When the projectile has partially perforated the plate (and mushroomed in the process), adiabatic shearing becomes highly likely if shear resistance is low. If shear resistance is high, the projectile would tend to bend and stretch the plate locally under balanced biaxial tension and this important deformation mode is identical as through-thickness compression. Thus, it appears that when



COMPRESSION MODE  
( $d' \leq t$ )



SHEAR MODE  
( $d' \geq 2t$ )

Figure 6

strength in both of these deformation modes is high, ballistic limit is likely to be high also, which is the case with the mixed  $(111) \langle 112 \rangle$  and  $(112) \langle 110 \rangle$  textures. Note that Hu et al.<sup>(1)</sup> reported increasing ballistic limit with increasing components of this mixed texture.

#### Possible Failure Modes

As far as failure modes are concerned,  $(100) \langle 023 \rangle$  texture, by virtue of its strength in shear and weakness in compression, is likely to promote bending around hole giving rise to petaling. The presence of this texture is very weak in the reustenitized and quenched steel in this investigation to ascertain this. However, the recrystallized plates containing  $(110) \langle 001 \rangle$  texture was also extremely weak in texture intensity and therefore do not allow the verification of these predictions. The spalling type failures for the strong mixed  $(111) + (112)$  texture appears to be quite reasonable in view of its strong resistance to any of the easier failure modes. Naturally when the impact velocity is raised to such a high degree as to generate appropriate tensile and compressive waves, spalling occurs.

Based on the above reasoning, Table II can be constructed in a speculative manner. Since cube-on-face texture has high shear resistance and low compression resistance, it is most likely that it will fail by petalling, i.e. thinning out at the bottom and tearing. Cube-on-edge having a low shear resistance will probably fail by shear plugging. Cube-on-corner orientation is also likely to fail by shear plugging because of low shear resistance. However, since the  $(111)$  planes are parallel to the rolling plane, it is likely to delaminate as the plate fibers are subjected to compression or bending forces. Delamination is known to increase crack path tortuosity and thereby enhance the energy absorbed during fracture. This coupled with high compression resistance is expected to produce a high ballistic limit for this type of texture.



For the (112) <110> texture failure mode could still be shear plugging due to its low shear resistance, however, since (112) plane is only at  $19^{\circ}$  to the slip plane, some degree of delamination might occur as well. Thus, the ballistic limit would possibly be moderate to high for this texture. For both cube-on-face and cube-on-edge textures, the absence of delamination might cause only a moderate ballistic limit. For all of these textures, however, back spalling could be initiated to sufficiently high projectile velocities.

TABLE II

<u>Texture</u>	<u>Possible Failure Type</u>	<u>Ballistic Limit</u>
Cube-on-face (100) < 001 > (100) < 023 >	Petalling	Moderate
Cube-on-edge (110) < 001 >	Shear Plugging	Moderate
Cube-on-corner (111) < 112 >	Shear Plugging Delamination	High
(112) < 110 >	Shear Plugging Delamination	Moderate to High

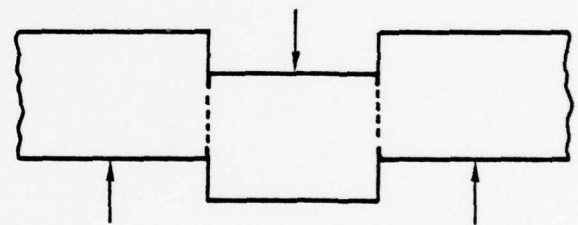
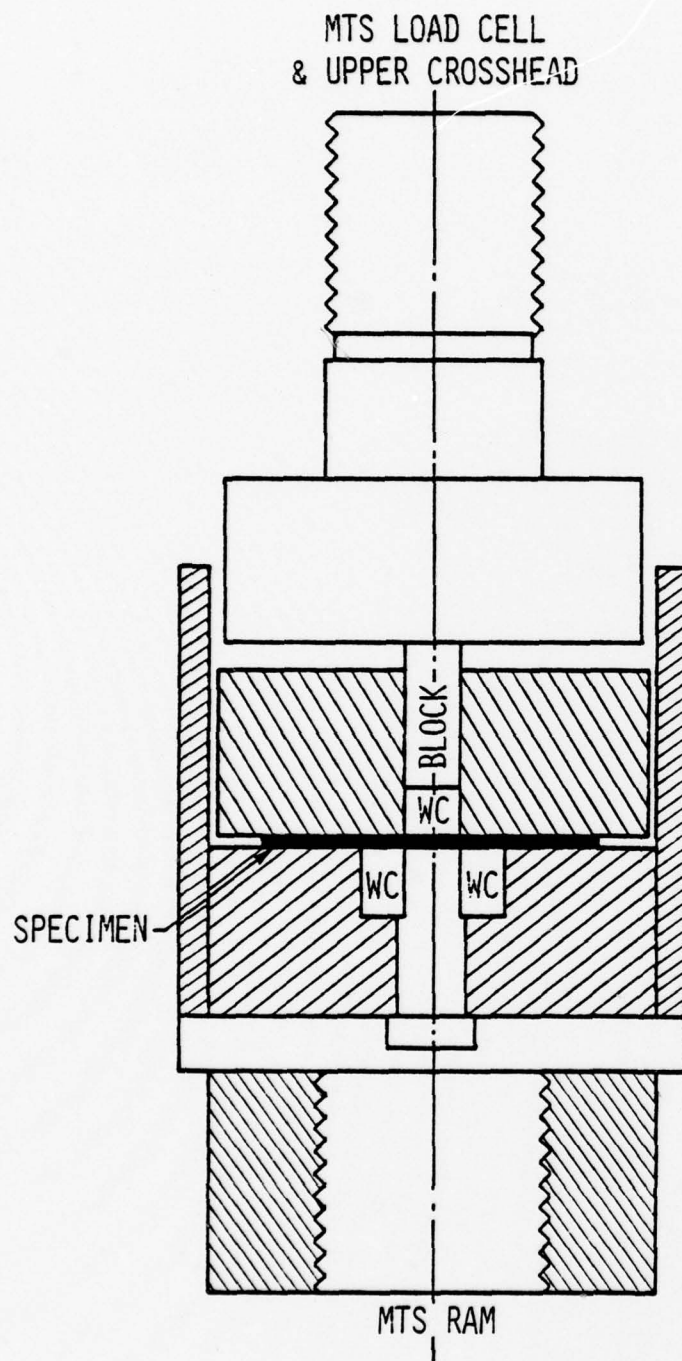


EXPERIMENTAL WORK

Shear strength does appear to be an important part of the ballistic perforation problem. It was decided that to provide comparisons with the calculations just presented as well as to develop some independent measures of shear strength for armor plates, planar shear tests be conducted. The test would simulate the cutting action of plate shears used in the industry and maintain a small enough clearance so as to maximize the shear forces and reduce both the tensile and compressive forces.

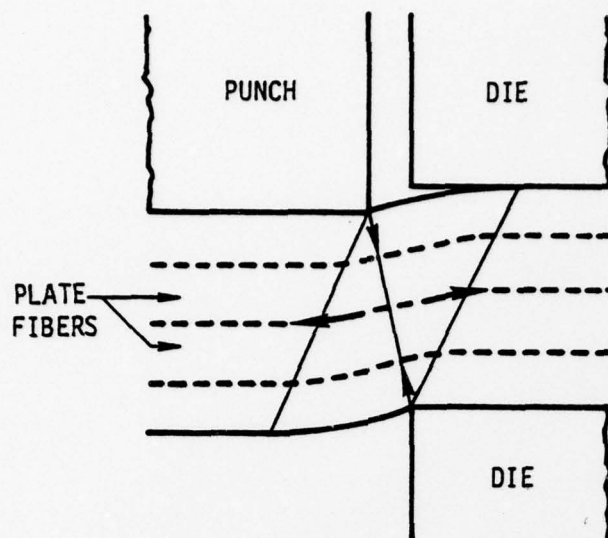
A test fixture shown schematically in Fig. 7 was constructed to shear  $\frac{1}{2}$ " wide strips of sheets. The lower part of the fixture holds two 0.6" wide tungsten carbide blocks 0.504" apart in a brass block and is attached to the MTS ram. A strip specimen, typically 0.08" thick by 0.5" wide by 3" long, is properly centered on the shearing blocks and held between the bottom part and a top circular plate by screws. This top plate also has a rectangular hole that acts as a guide for the central 0.5" wide tungsten carbide shearing block. The doubly supported shearing test is sketched on the right. The clearance between each pair of shears of 0.002" and the shear edges are prepared to be as sharp as possible.

The upper platen is attached to the upper crosshead of the MTS machine through a load cell (up to 50,000 lbs). It rests on the central carbide block while the ram is moved up to start the shearing action. The test is run under stroke control at speeds of 0.005 in/sec to 0.5 in/sec, and a load vs ram displacement plot is maintained. A typical load displacement plot for armor plates consists of a linearly (elastic) rising region followed by a non-linear portion, exhibiting a load maximum and a catastrophic fracture after the load has dropped somewhat (Fig. 8). A measure of yield strength is obtained at the end of the linear elastic region. Some amount of strain hardening also occurs prior to the load maximum. A schematic diagram of the mechanics of the shear test is also illustrated in Fig. 8. While there is



SHEAR TEST

Figure 7



SC5122.7 FR

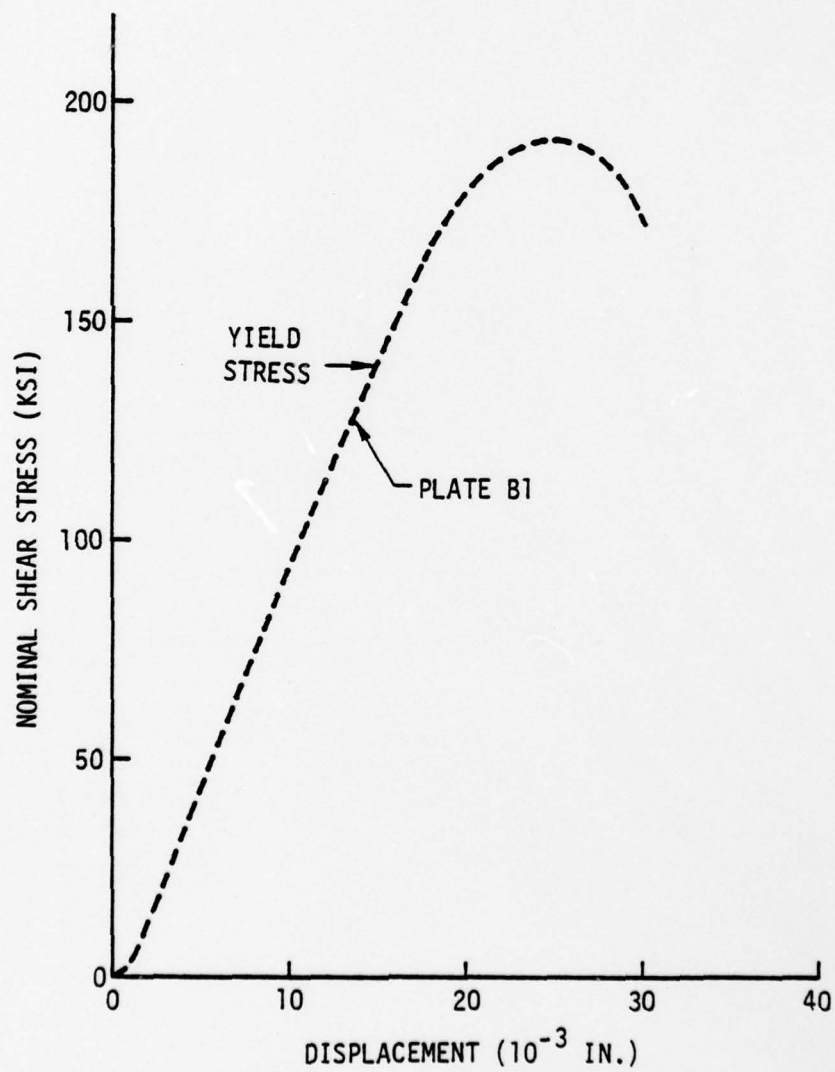


Figure 8

SC78-966

some plane strain tension of the material held within the clearance, the superimposition of plane strain compression between plantens provides an overall state very close to pure shear.

### Specimens

Table III lists the test plates of armor steel that were prepared by U.S. Steel<sup>(1)</sup> and supplied to us by the Army Materials and Mechanics Research Center. These plates have varying intensities of (111)+(112) texture as noted in the Table. They are all nominally 0.50" thick plates out of which 0.5" wide by 3" long pieces were cut off by using a diamond saw. The cuts were made at 0, 30, 60 and 90° to the rolling direction. From 2-3 blocks cut for each direction, slices were cut at angles of 0, 10 and 20° to the top face of the plate. These slices represent, respectively, the impact obliquities of the same amount. They were further surface ground for parallel faceting and a nominal thickness of 0.080". Samples were tested in the shear fixture already described and the 3" length provided us with 3 measurements to be made on each strip. The yield strength from the three tests were averaged and the results were not found to vary with test speed.

TABLE III

5% Ni-Steel (Quenched) Plated to be Used in This Program

Plate Number	Thickness (inches)	Percent Reduction	I Max
705-A1	.489	60	3.8
-B1	.502	70	5.1
-C2	.502	80	6.6
-D1	.492	90	9.1
717-D2	.497	90	7.2

The shear test was performed on all five plates in Table III. (These steels were quenched from <sup>hot-</sup>rolling temperature.) The shear strength plots as a function of angle in the plane of the plots are shown in Fig. 9. The



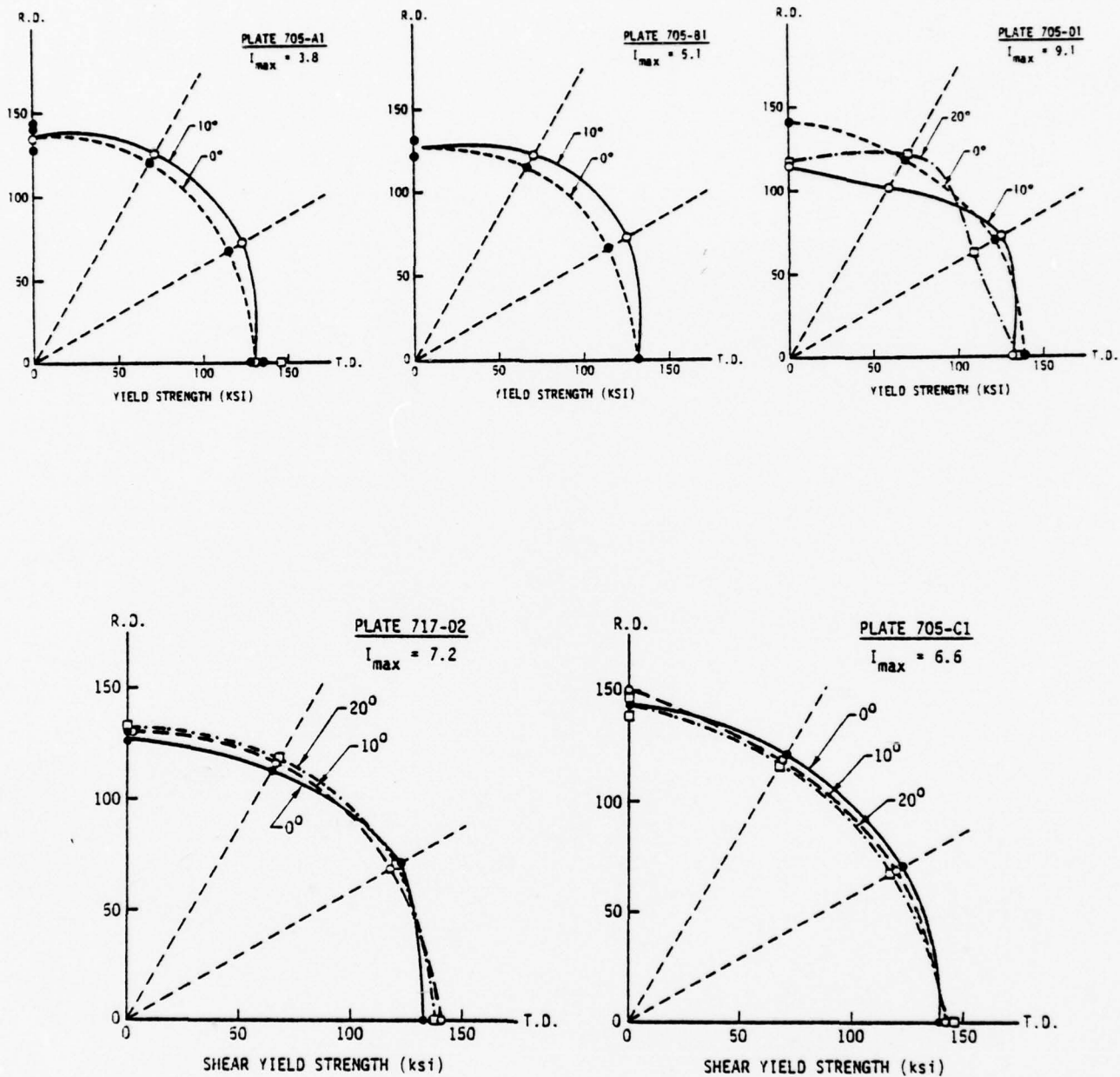


Figure 9

results include samples cut at 0, 10 and 20° to this plane (i.e., angles of 90, 80 and 70° to the plate normal, respectively). The plotted values represent strips in these directions with shear actually normal to those directions.

The yield strengths in through-thickness compression tests were determined for plates A1, B1, C1 and D1 from the load-displacement plots in a manner similar to the determination of shear yield points. These samples were 0.2" dia and 0.4" long. Samples were tested in compression using polyethylene and oil for lubrication between the specimen and the platens. Yield strengths were measured from these tests. Since the shear instability limited the uniformity of deformation, the maximum load and the details of load-deflection plot were not very useful. Figure 10 shows a plot of through-thickness yield strength as a function of texture intensity for the different plates. Even though the increase is modest, a clear increasing trend in strength is observed with increasing intensity. Approximately a 10% strength increase has been seen in going from plate A1 to D1. Table IV gives these yield strength values which are somewhat lower than those determined at U.S. Steel Laboratory for the same plates.

TABLE IV

Strength Properties of Hot-Rolled and Quenched 5% Ni Steel plated

Plate Identification	Rolling Reduction (%)	Texture Intensity $I_{max}$	Compressive Yield Strength (Ksi)	Shear Yield Strength (Ksi)	Estimated Value of $R^*$
705-A1	60	3.8	239.0	133 $\pm$ 3	1.11
705-B1	70	5.1	238.8	135 $\pm$ 3	1.06
705-C1	80	6.6	252.6	136 $\pm$ 2	1.22
705-D1	90	9.1	261.3	132 $\pm$ 5	1.45

\*Plastic Anisotropy parameter, R, calculated from the relation:  $\sigma_{shear} = \sqrt{1 + 2R} \sigma_{biaxial}$

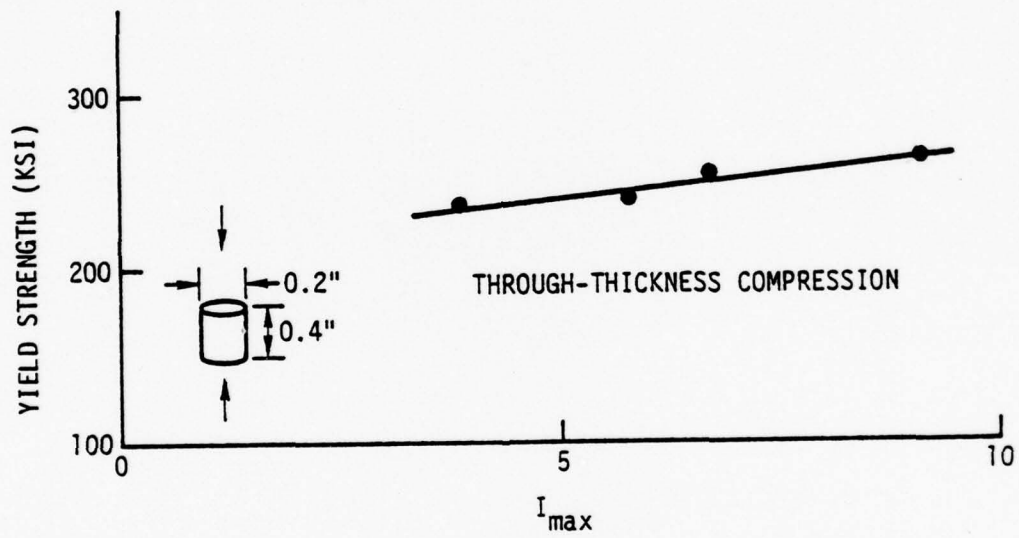


Figure 10

SC78-969



For an assessment of the energy absorbed in the shear test, the area under the load displacement plots were determined and normalized with respect to the cross-sectional area sheared through. This energy per unit area nearly represents energy/volume for comparison among different plates assuming the width of the shear zone to be the same. Figure 11 shows this absorbed energy as a function of shear yield strength for two of the plates tested. While the scatter in the data is very large, there is a mild upward trend indicating that if texture modification does increase the shear strength of the material, it is also likely to increase the ballistic perforation resistance.

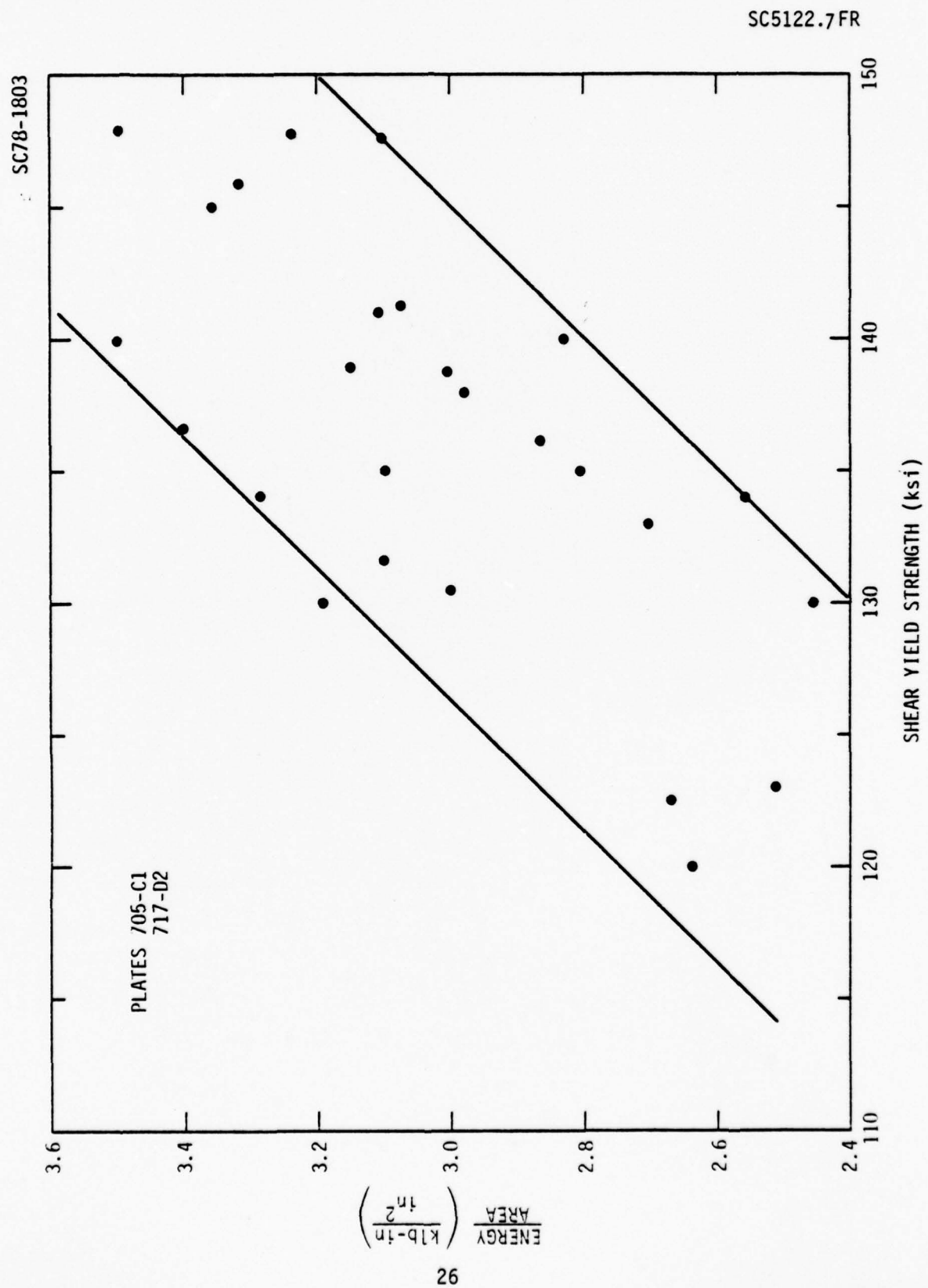


Figure 11

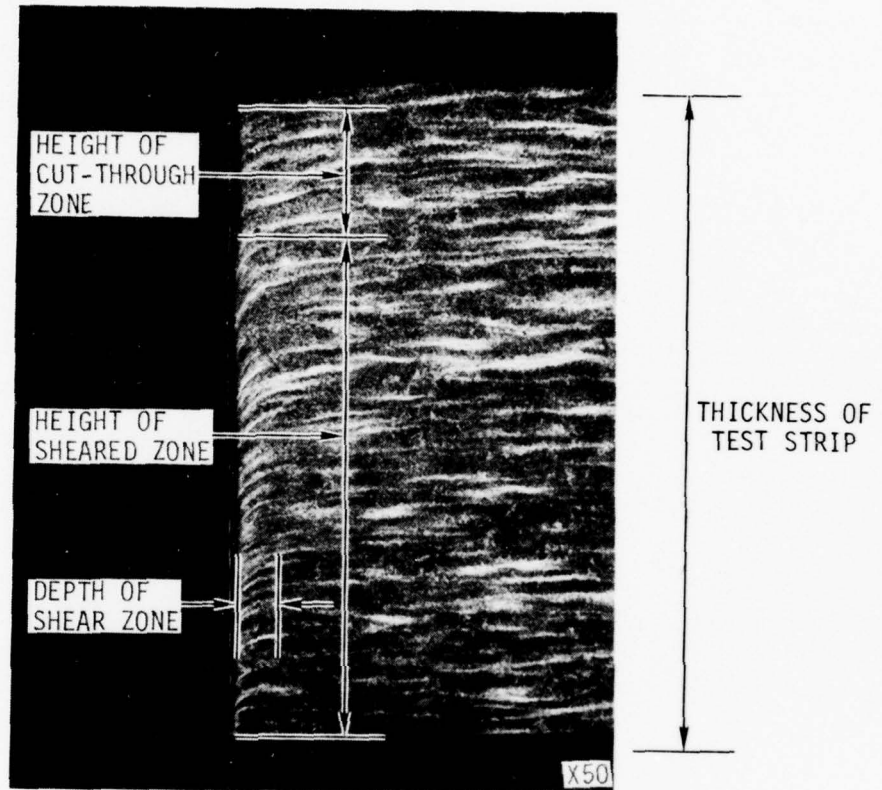
## RESULTS AND DISCUSSIONS

A micrograph of the sheared edge of a tested specimen is shown in Fig. 12. Near the top part of the strip where the punch essentially cuts through the material prior to the fast shear fracture zone, the fibers are bent less sharply near the edge compared to the rest of the plate thickness. This indicates somewhat of a departure from pure shear state near the top; however, since nearly 80% of the strip deforms by pure shear, this kind of test for determining shear strength appears to be justified. The most perfect test for pure shear is torsion of a thin-rolled tube which is rather difficult to perform from 0.5" thick rolled plate stock of hardness  $R_c 55$ . Another feature observed from Fig. 12 is that the depth of zone inside the material that appears to have taken part in the shear deformation is about 0.005" compared to a strip thickness of 0.077". This zone depth compares well with the clearance between shears which is also 0.005". While this zone depth depends on the strain hardening capacity of the material, its small size indicates the effectiveness of the shear test. In agreement with the present observation, Daneshi and Harding<sup>(2)</sup> had found in high speed punching of steel plates that the top part of the plate exhibited little shear strain, while deeper into the plate shear strain increased.

Figure 13 shows the side view of a sheared edge. Application of a 0.02" square grid on the surface prior to the test reveals the intense shear deformation. Measurement of the grid afterwards shows that deformation is pure shear within the boxed area with a local shear strain of about 0.8-1.0 at fracture, which indicates that shear failure is by no means a brittle mode.

The shear strength plots as a function of angle in the plane of the plots are shown in Fig. 9. The results include samples cut at 0, 10 and 20° to this plane (i.e., angles of 90, 80 and 70° to the plate normal, respectively). The plotted values represent strips in these directions with shear actually normal to those directions.

SC5122.7FR



SC78-967

Fig. 12

SC5122.7FR

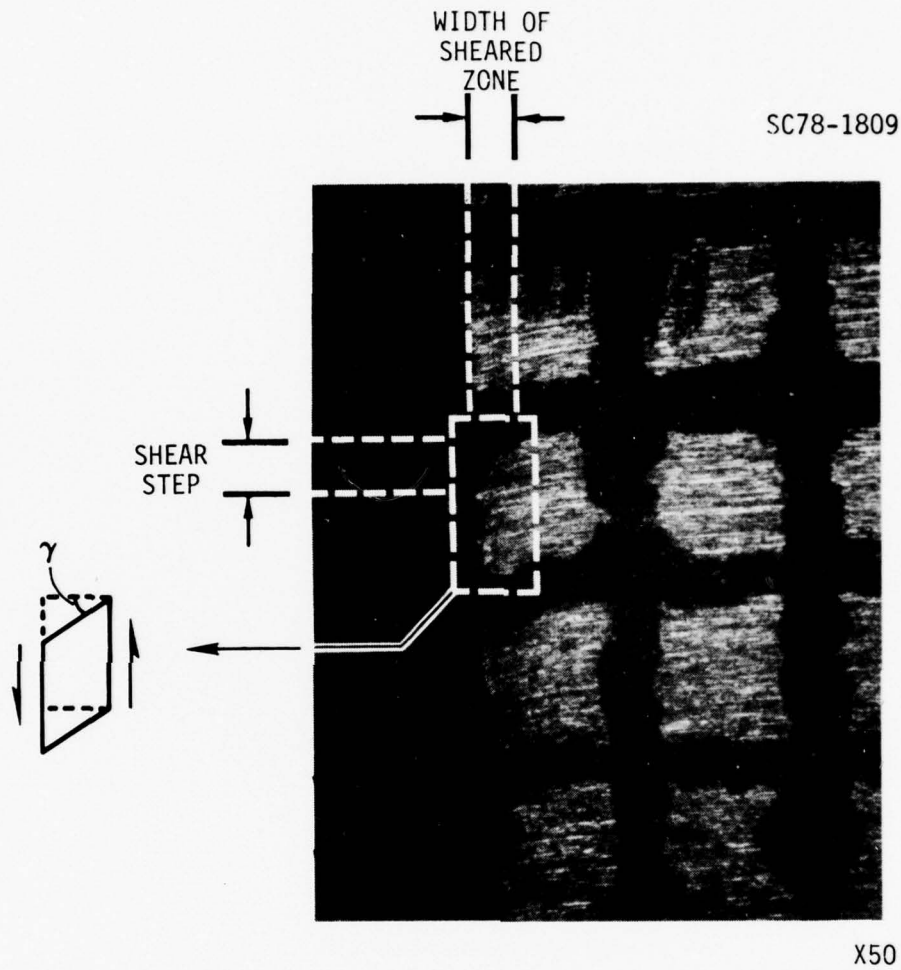


Fig. 13



Some variation is observed in tests out of the plane, as shown in Fig. 9; however, this is not very large. The theoretical results indicated that somewhat higher shear strength values might be expected at inclinations of  $20^{\circ}$  to the plate normal. However, the scatter in the observed data may be large enough to obscure such a trend. Because the maximum stress data show essentially the same behavior as shear yield data they are not plotted here. Variations as a function of angle within the plane of the plate or out of plane are also very small.

The comparison among the shear yield strength of all five plates is shown in Fig. 14 by plotting an average curve for each. Again, no significant shear strength variation is observed among them. An average shear yield strength for all of the plates is around 130-135 Ksi, while their maximum shear strength averages around 175 Ksi. The invariance of shear strength within the experimental scatter band agrees well with theoretical predictions. Between texture intensities of 3.8 and 9.1, shear resistance variation of 5% or less might be expected on the basis of the theory.

Through-thickness compression tests on all four armor plates of the 705 plate series indicated an increasing strength with increasing texture intensity. An increase in intensity from 3.8 to 9.1 gave rise to a strength increase from 238 to 261 Ksi. Such an increase was predicted from theoretical calculations presented in the last quarter, and corresponds to an increase in plastic anisotropy parameter  $R$ , by 30%. Ballistic perforation resistance appears to be strongly related to both through-thickness resistance and to some degree, on the shear yield strength.

SC5122.7FR

SC78-1802

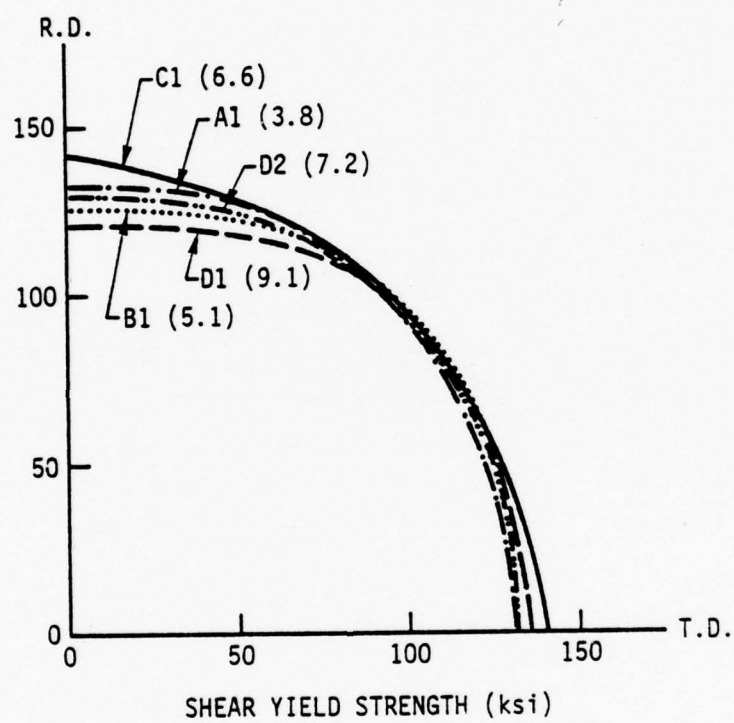


Figure 14

Figure 15 shows the scanning electron micrographs of fracture surfaces of the shear specimens. Figure 15(a) shows a shear-cut zone on top followed by a fast fracture zone at the bottom. Referring to the right side illustration in Fig. 3, when the crack depth below the shearing edge and stress concentration are large enough, crack propagation occurs rapidly leading to fracture. Thus, Fig. 15(a) indicates that nearly 80% of the fracture surface represents a fast shear fracture zone and justifies the use of the present test. Figure 15(b) illustrates that void opening takes place during the cutting process, so it is partially ductile in character. The fracture in Fig. 15(c) appears to be of a mixed type, with combinations of ductile, dimple type and relatively smooth type.

Finally, Fig. 16 shows a macrosection of a hole produced by the impact of a projectile on an armor plate from Ref. 1. This plate had the highest reported intensity of (111) + (112) textures. While there are some areas of back spalling, considerable amount of delamination is observed as expected for this texture. In agreement with our previous finding, the (111) planes parallel to the plane of the plate appear to absorb a great deal of impact energy by increasing the crack path tortuosity. No special directionality in the plane of the plate is observed here. This is believed to be the reason for its high ballistic limit. Also, this motivates the projectile to seek an easier shear path, such as another (111) plane inclined at  $70^\circ$  to the plane of the plate. This provides a rationale for the non-normal exit direction of the projectile. Figure 17 shows micrographs of elongated voids developing in the banded martensitic structure of the previous sample. The voids are elongated, usually in between two bands, and a number of them join up to cause delamination. Also adiabatic shear zone (white in Fig. 17b) develop either along the bands or about  $70^\circ$  to the bands and join the regions between elongated voids.

SC5122.7FR

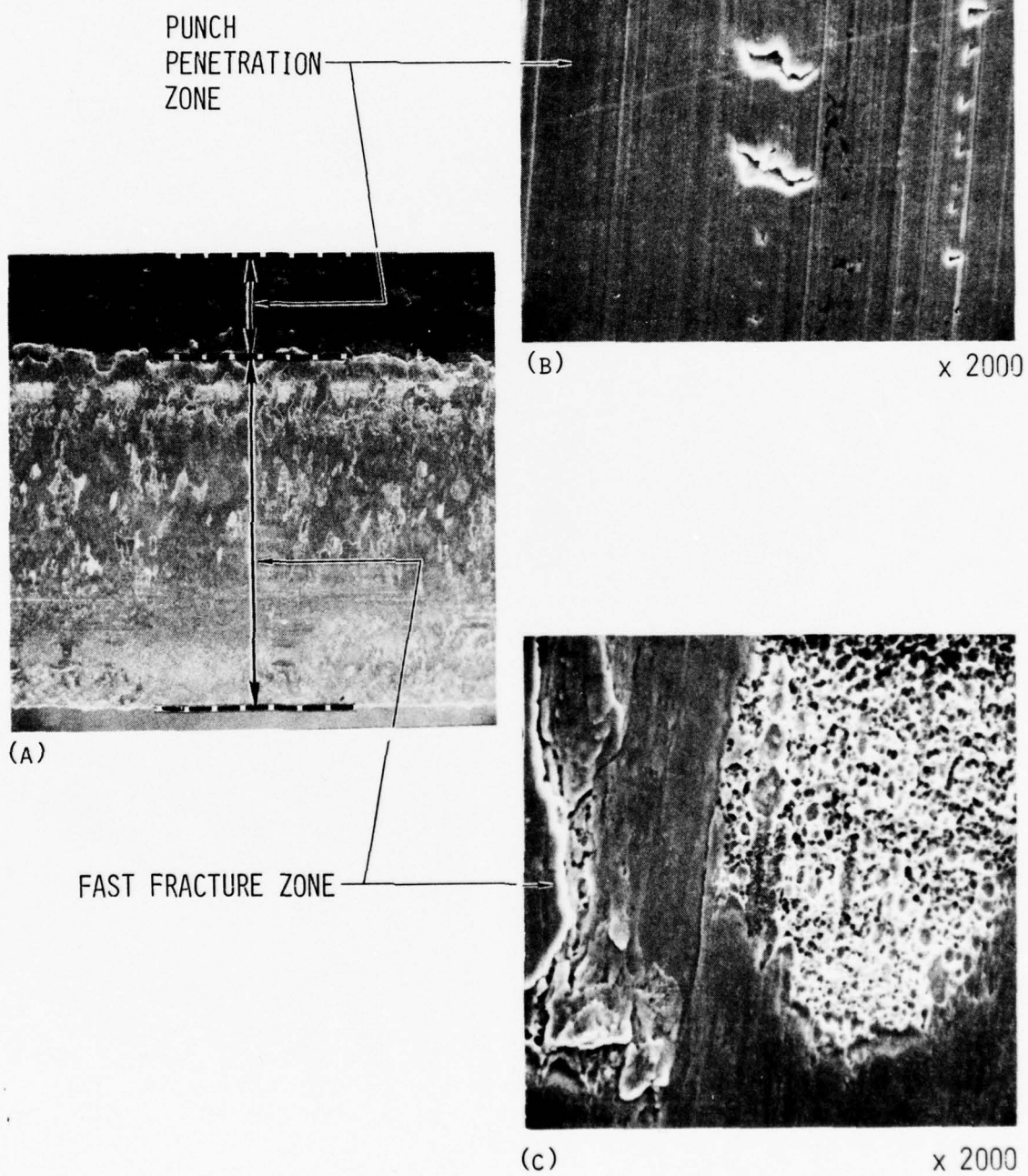
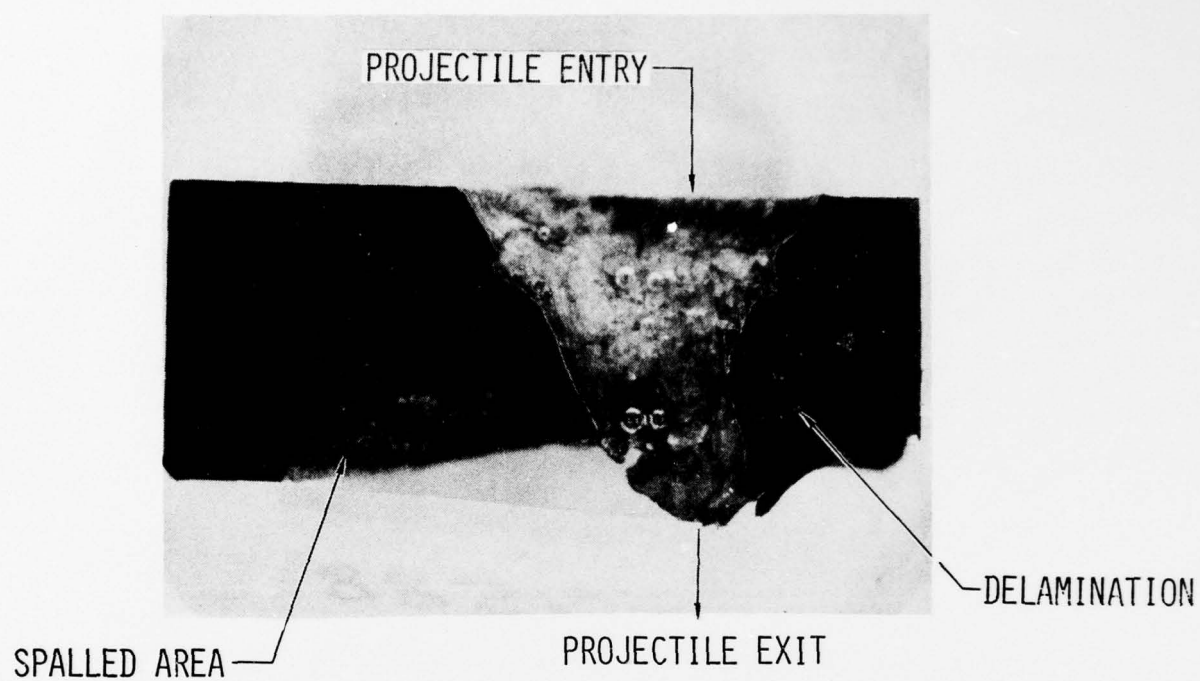


Fig. 15





SC78-102

Fig. 16



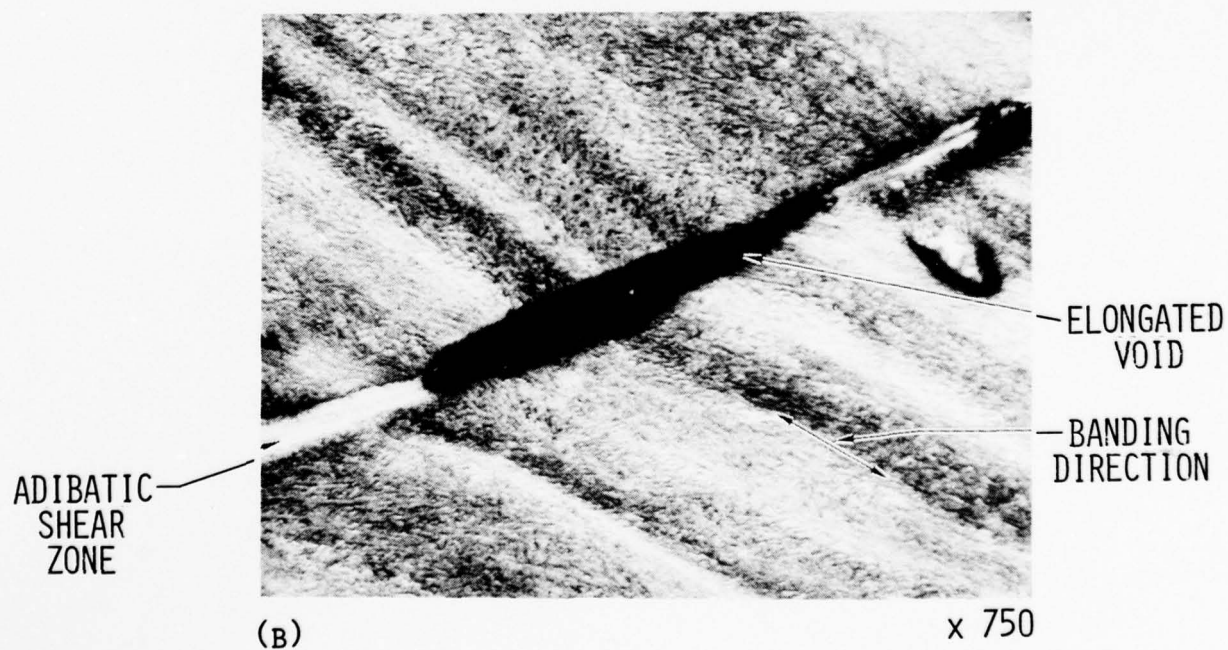
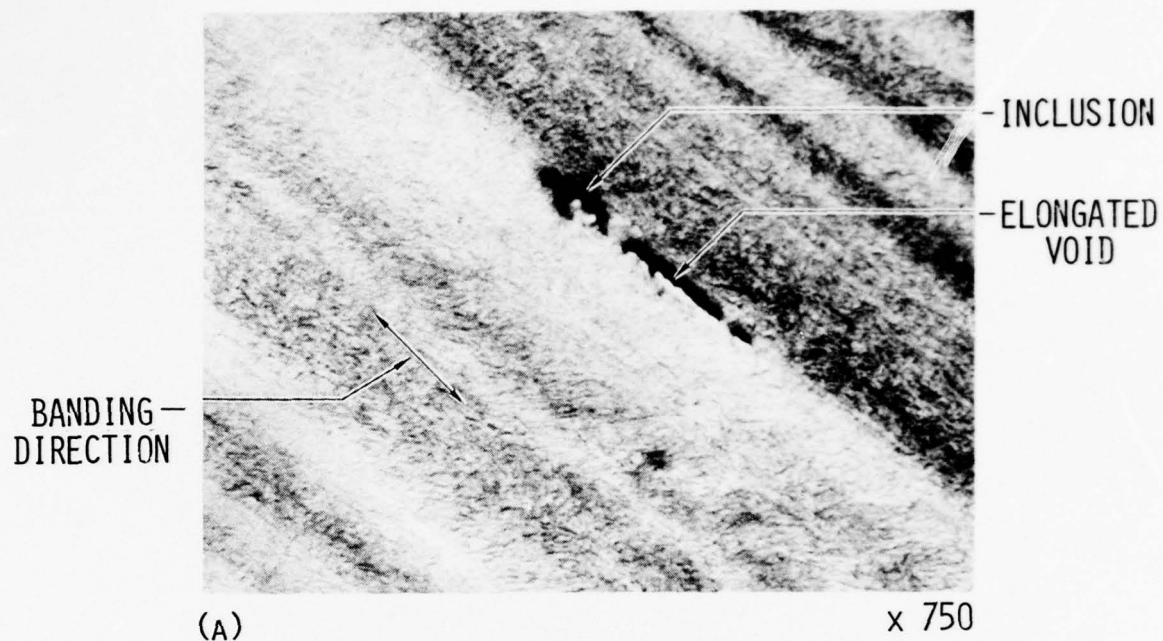


Fig. 17

SC78-131

### SUMMARY AND CONCLUSIONS

In order to rationalize the improvement in ballistic penetration resistance with increasing intensity of (111) and (112) textures in quenched 5% Ni steel plates,<sup>(1)</sup> a detailed theoretical study of texture strengthening has been carried out in conjunction with experimental shear tests on the above material. Since the armor plate behaves in a rigid manner initially during the supersonic impact by the projectile, the first increment of deformation is by pure compression. Resistance to through-thickness compression is therefore the most important criterion for ballistic perforation resistance. Subsequent deformation can be either by shear (as in the plugging mode) or by balanced biaxial tension (as in the petalling mode). Resistance to shear is therefore also important. When the resistances to both compression and shear are high, the ballistic limit becomes very high, and there is no alternative but back spalling to start. Back spalling can occur in any of the other plates as well provided the projectile velocity is large enough to generate the tensile and compressive waves of the appropriate magnitudes. The conclusions from the theoretical calculations of ideal texture strength and shear experiments are given below:

- (1) Cube-on-edge, (110) <001>, and cube-on-corner, (111) <112> textures are found to be approximately 25% stronger in through-thickness compression and somewhat weaker in shear as compared to the random texture.
- (2) (112) <110> texture shows nearly the same resistance in compression and shear as the random texture.
- (3) Cube-on-face, (100) <001>, and (100) <023> have nearly 40% greater resistance to shear deformation, but 30% lower resistance to compression in comparison to random texture.

- (4) Through-thickness compression resistance is independent of direction in the plane of the plate; however, some of the ideal textures exhibited mirror plane symmetry in shear resistance about  $45^{\circ}$  directions.
- (5) Planar shear tests indicated modest variation of strength (5%) with angles to the plane of the plate, and within the plane of the plate. These results agree with theoretical predictions. Average shear yield strengths were found to be around 130-135 Ksi, while ultimate shear strengths are around 175 Ksi.
- (6) Through-thickness compression tests on all four armor plates of the 705 plate series indicate an increasing strength with increasing texture intensity. An increase in intensity from 3.8 to 9.1 gave rise to a strength increase from 238 to 261 Ksi. Such an increase was predicted from theoretical calculations, and corresponds to an increase in plastic anisotropy parameter  $R$ , by 30%. The 10% strength increase compares with a rise in ballistic limit of about 11%.<sup>(1)</sup>

REFERENCES

1. Hsun Hu, G.R. Speich and R.L. Miller, AMMRC Report CTR 76-22, July 1976.
2. Hsun Hu, AMMRC Report CTR77-19, July 1977.
3. G.I. Taylor, J. Inst. Metals, Vol. 62, 1938, p. 307; S. Timoshenko, 69th Anniversary Volume, P. 218, MacMillan Co., New York, 1938.
4. J.F.W. Bishop and R. Hill, Phil. Mag., Vol. 42, 1951, p. 1298.
5. W.F. Hosford and W.A. Backofen, Fundamentals of Deformation Processing, W.A. Backofen et al., eds. p. 259-98, Syracuse University Press, New York, 1964.
6. G.Y. Chin and W.L. Mammel, Trans. Met. Soc., AIME, Vol. 239, Sept. 1967, p. 1400; also G.Y. Chin, W.L. Mammel and M.T. Dolarn, Trans. Met. Soc. AIME, Vol. 239, 1967, p. 1111.
7. G.Y. Chin and B.C. Wonsiewicz, Met. Trans., Vol. 1, 1970, p. 551.
8. G.Y. Chin, W.F. Hosford and D.R. Mendorf, Proc. Roy. Soc. A309, 1969, p. 433.
9. R.F. Recht and T.W. Ipson, Trans. ASME, Sept. 1963, p. 384.
10. W.F. Hosford and G.Y. Chin, Trans. AIME-TMS, Vol. 245, 1965, p. 877.
11. H.R. Piehler and W.A. Backofen, Ph.D. Thesis, M.I.T. Cambridge, Mass. 1967.
12. G. H. Daneshi and J. Harding. J. Phys. D: Appl. Phys., 7 (1974) 404.



APPENDIX

The influence of impact obliquity is shown in Figs. 1-A through 6-A. The important effect for the mixed (111) + (112) texture is that strength in compression diminishes, while the strength in shear increases with departures from normality. The overall penetration resistance may not be significantly influenced. The calculated values are for unit material thickness in the impact direction. Comparison with experimental results would require correcting for the increased thickness due to inclination.



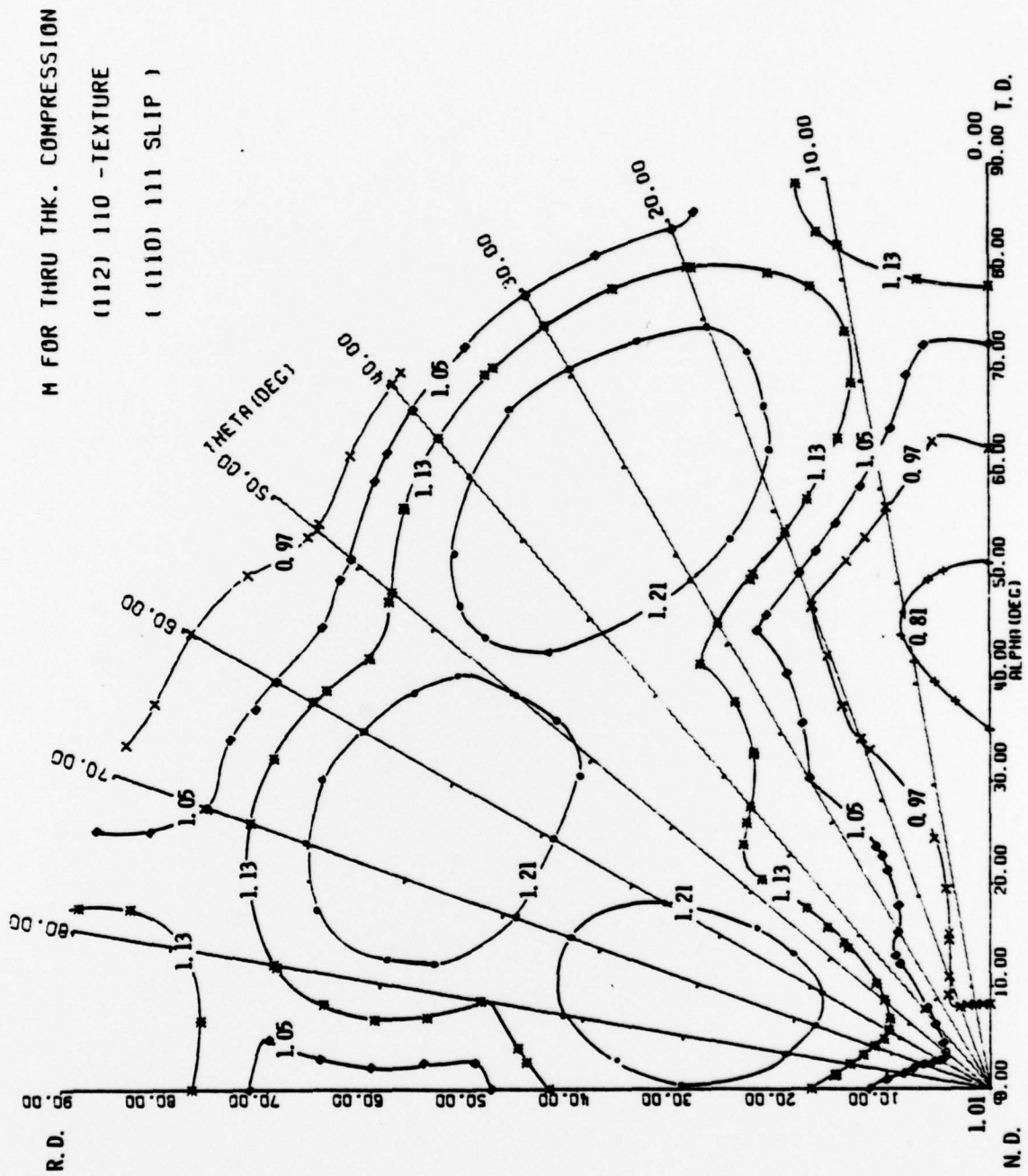


Figure 1-A

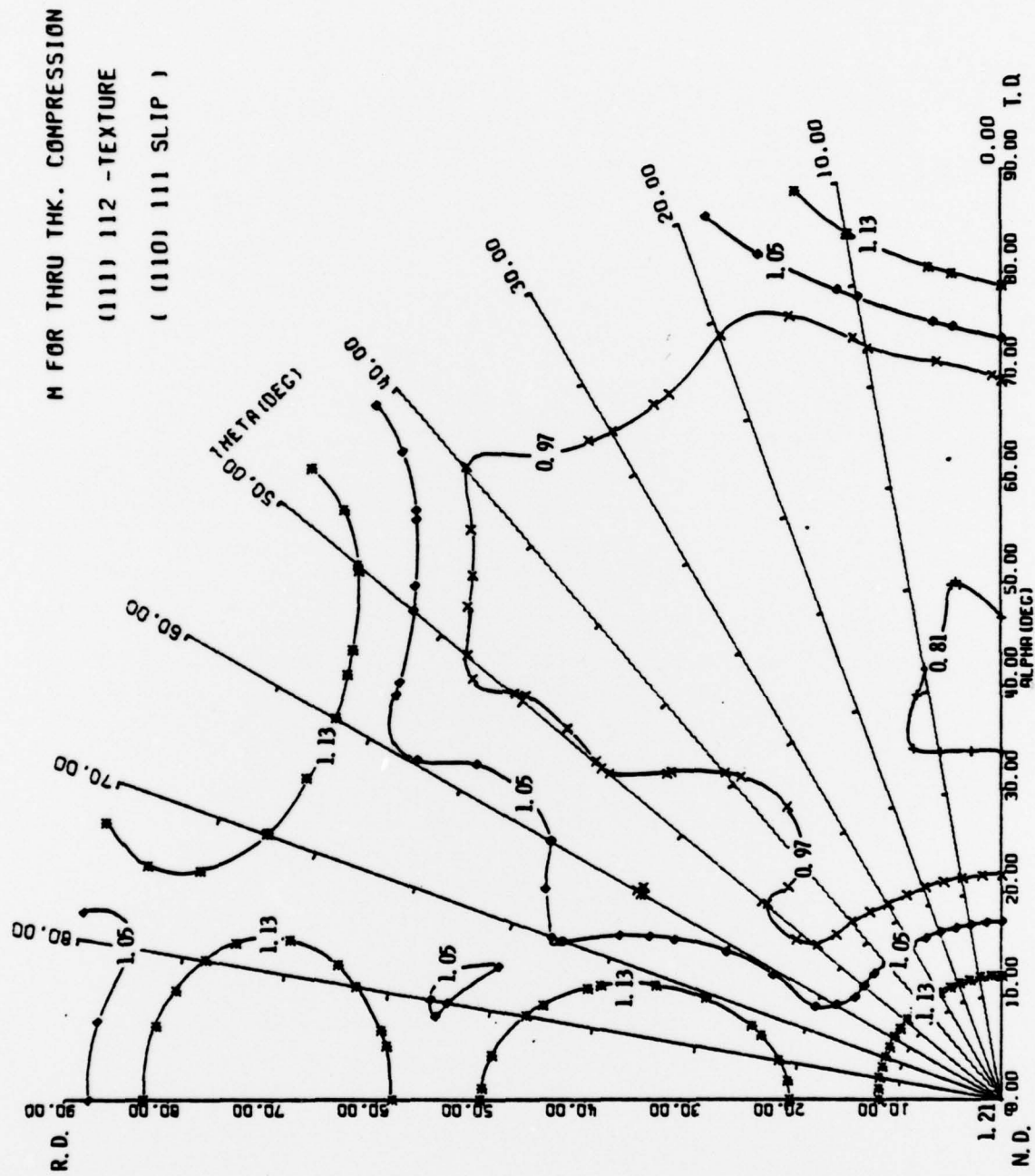


Figure 2-A

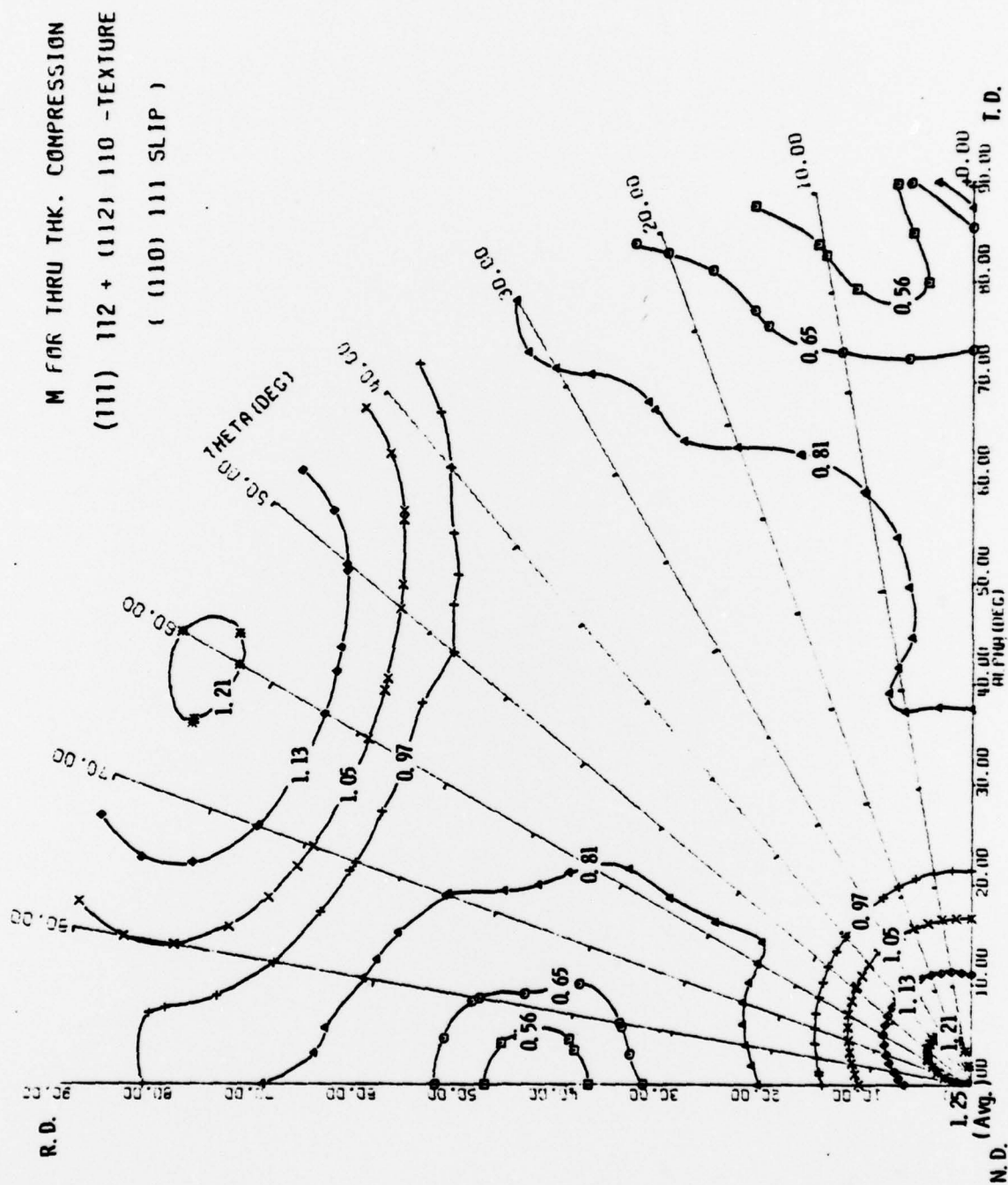


Figure 3-A

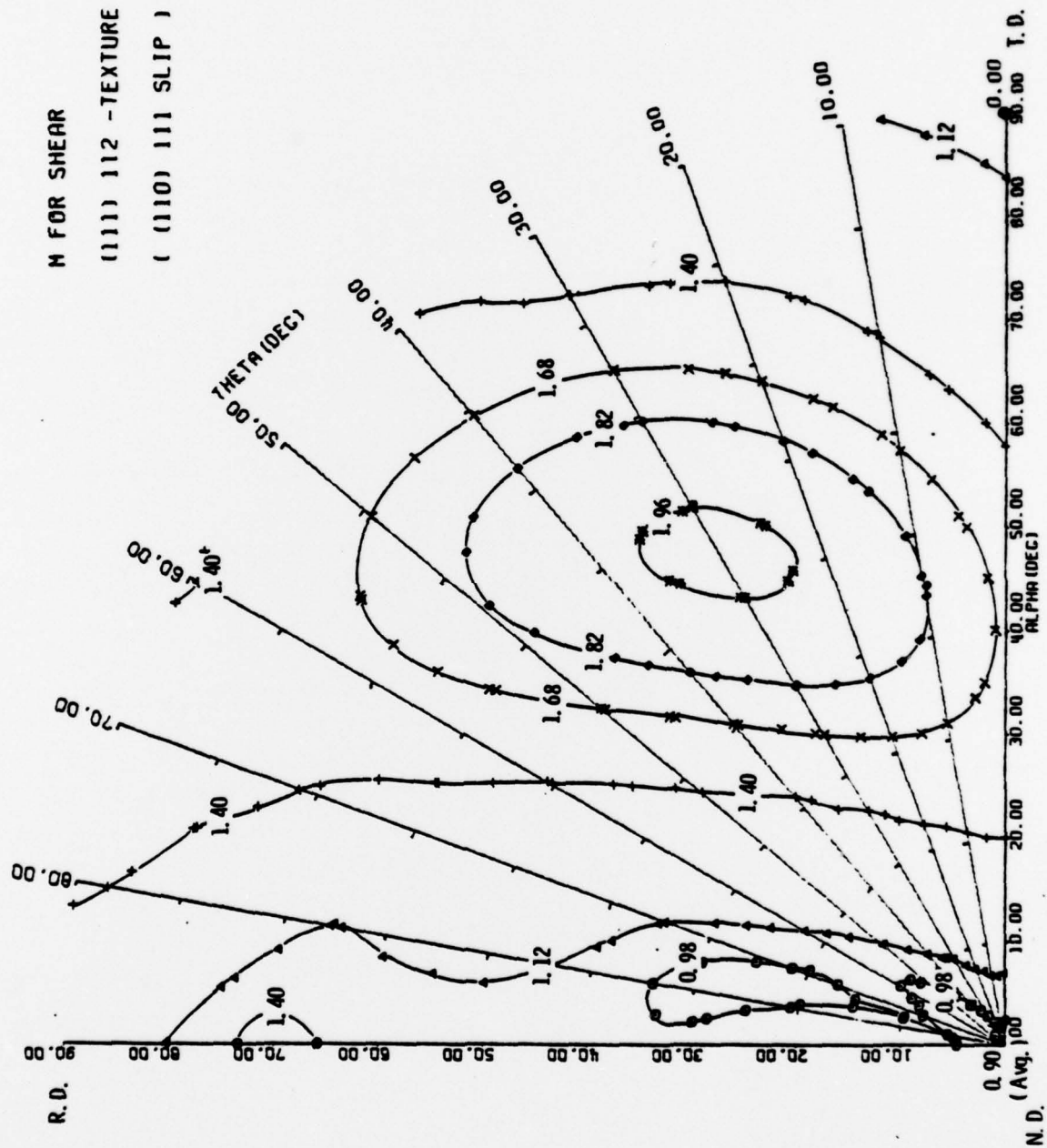


Figure 4-A



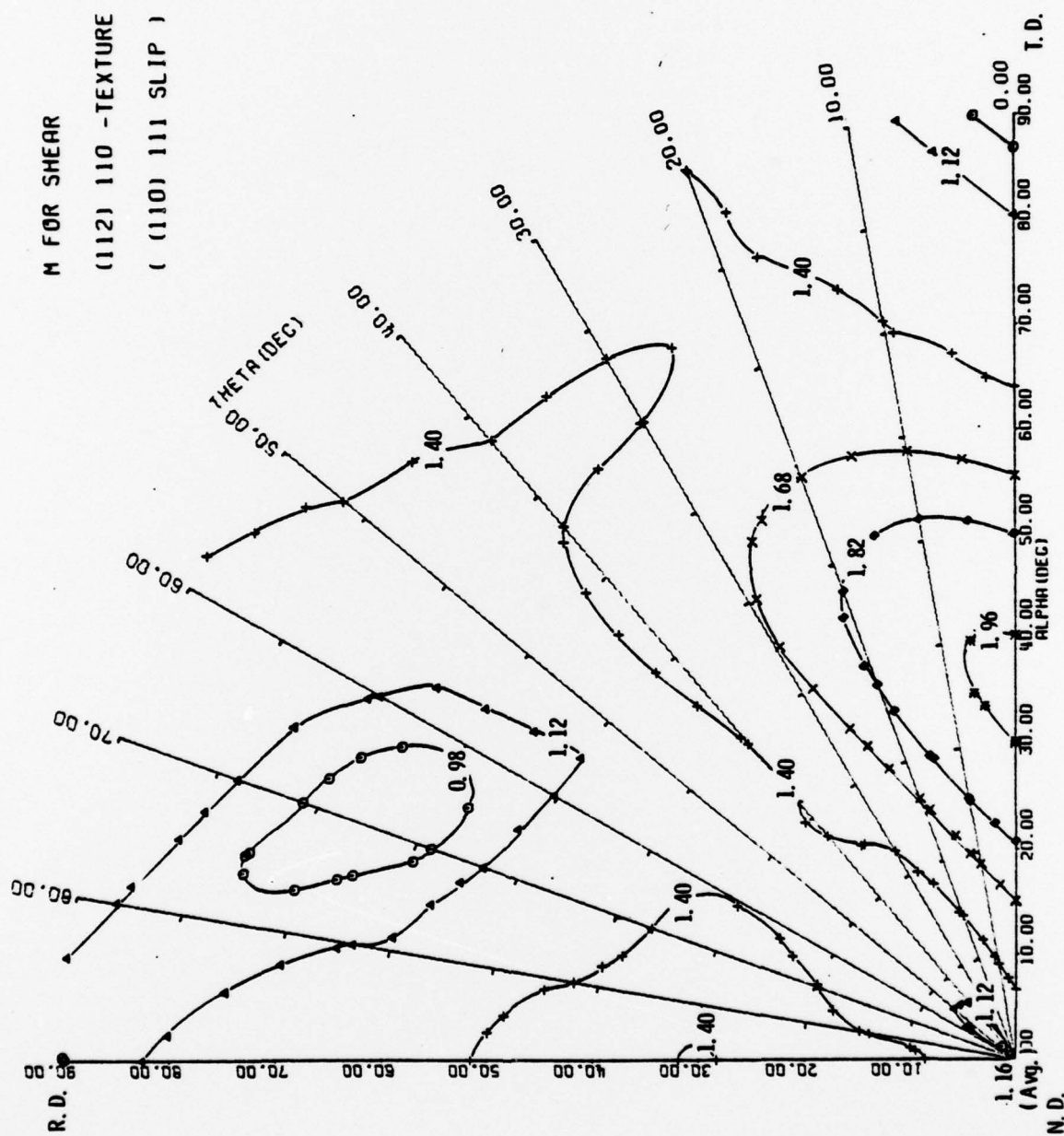


Figure 5-A



SC5122.7FR

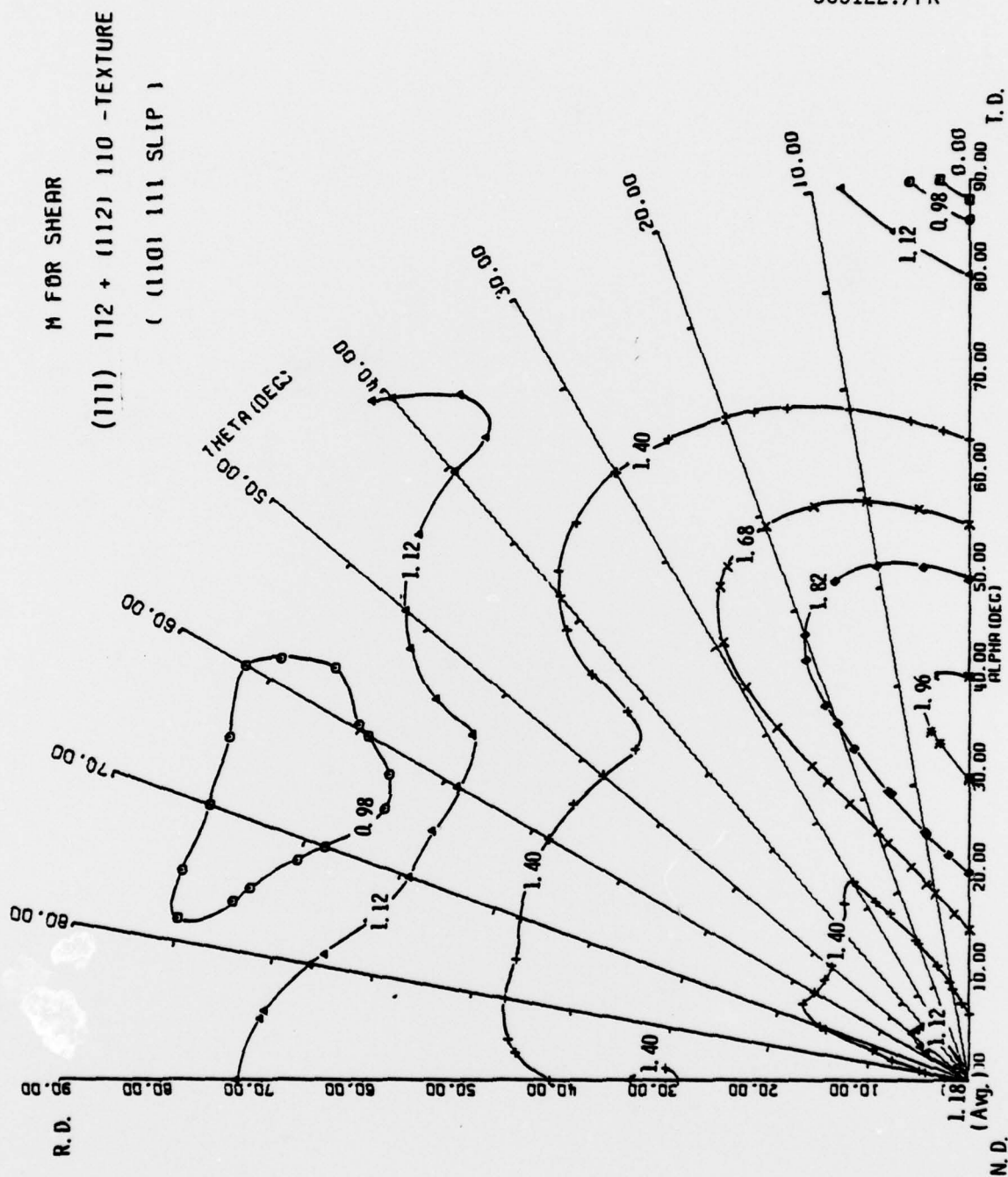


Figure 6-A

ACKNOWLEDGMENTS

We would like to thank Prof. W. F. Hosford of University of Michigan, Ann Arbor, Michigan for his help with the computer program for calculating Taylor factors. The work of Mr. P. Sauers in connection with the specimen preparation and Mr. R. Spurling in connection with the metallography is greatly appreciated.

# DISTRIBUTION LIST

No. of Copies	To
1	Office of the Director, Defense Research and Engineering, The Pentagon, Washington, D. C. 20301
12	Commander, Defense Documentation Center, Cameron Station, Building 5, 5010 Duke Street, Alexandria, Virginia 22314
1	Metals and Ceramics Information Center, Battelle Columbus Laboratories, 505 King Avenue, Columbus, Ohio 43201
	Chief of Research and Development, Department of the Army, Washington, D. C. 20310
2	ATTN: Physical and Engineering Sciences Division
	Commander, Army Research Office, P. O. Box 12211, Research Triangle Park, North Carolina 27709
1	ATTN: Information Processing Office
	Commander, U. S. Army Materiel Development and Readiness Command, 5001 Eisenhower Avenue, Alexandria, Virginia 22333
1	ATTN: DRCLDC, Mr. R. Lentner
	Commander, U. S. Army Electronics Command, Fort Monmouth, New Jersey 07703
1	ATTN: DRSEL-GG-DD
1	DRSEL-GG-DM
	Commander, U. S. Army Missile Command, Redstone Arsenal, Alabama 35809
1	ATTN: Technical Library
1	DRSMI-RSM, Mr. E. J. Wheelahan
	Commander, U. S. Army Armament Command, Rock Island, Illinois 61201
2	ATTN: Technical Library
1	DRSAR-PPW-PB, Mr. Francis X. Walter
	Commander, U. S. Army Natick Research and Development Command, Natick, Massachusetts 01760
1	ATTN: Technical Library
	Commander, U. S. Army Satellite Communications Agency, Fort Monmouth, New Jersey 07703
1	ATTN: Technical Document Center
	Commander, U. S. Army Tank-Automotive Research and Development Command, Warren, Michigan 48090
2	ATTN: DRDTA, Research Library Branch
	Commander, White Sands Missile Range, New Mexico 88001
1	ATTN: STEWS-WR-VT

No. of  
Copies

To

Commander, Aberdeen Proving Ground, Maryland 21005  
1 ATTN: STEAP-TL, Bldg. 305  
1 DR. G. L. FILBEY, DRXER-TB

Commander, Dugway Proving Ground, Dugway, Utah 84022  
1 ATTN: Technical Library, Technical Information Division

Commander, Edgewood Arsenal, Aberdeen Proving Ground, Maryland 21010  
1 ATTN: Mr. F. E. Thompson, Dir. of Eng. & Ind. Serv., Chem-Mun Br

Commander, Frankford Arsenal, Philadelphia, Pennsylvania 19137  
1 ATTN: Library, H1300, Bl. 51-2  
1 SARFA-L300, Mr. J. Corrie

Commander, Harry Diamond Laboratories, 2800 Powder Mill Road,  
Adelphi, Maryland 20783  
1 ATTN: Technical Information Office

Commander, Picatinny Arsenal, Dover, New Jersey 07801  
1 ATTN: SARPA-RT-S

Commander, Redstone Scientific Information Center, U. S. Army Missile  
Command, Redstone Arsenal, Alabama 35809  
4 ATTN: DRSMI-RBLD, Document Section

Commander, Watervliet Arsenal, Watervliet, New York 12189  
1 ATTN: SARWV-RDT, Technical Information Services Office

Commander, U. S. Army Foreign Science and Technology Center,  
220 7th Street, N. E., Charlottesville, Virginia 22901  
1 ATTN: DRXST-SD2

Director, Eustis Directorate, U. S. Army Air Mobility Research and  
Development Laboratory, Fort Eustis, Virginia 23604  
1 ATTN: Mr. J. Robinson, SAVDL-EU-SS

Librarian, U. S. Army Aviation School Library, Fort Rucker, Alabama 36360  
1 ATTN: Building 5907

Commander, U. S. Army Environmental Hygiene Agency, Edgewood Arsenal,  
Maryland 21010  
1 ATTN: Chief, Library Branch

Commandant, U. S. Army Quartermaster School, Fort Lee, Virginia 23801  
1 ATTN: Quartermaster School Library

Naval Research Laboratory, Washington, D. C. 20375  
1 ATTN: Dr. J. M. Krafft - Code 8430  
2 Dr. G. R. Yoder - Code 6382



Number of  
Copies

To

Chief of Naval Research, Arlington, Virginia 22217  
1 ATTN: Code 471

Air Force Materials Laboratory, Wright-Patterson Air Force Base, Ohio 45433  
2 ATTN: AFML/MXE/E. Morrissey  
1 AFML/LC  
1 AFML/LLP/D. M. Forney, Jr.  
1 AFML/MBC/Mr. Stanley Schulman

National Aeronautics and Space Administration, Washington, D. C. 20546  
1 ATTN: Mr. B. G. Achhammer  
1 Mr. G. C. Deutsch - Code RR-1

National Aeronautics and Space Administration, Marshall Space Flight  
Center, Huntsville, Alabama 35812  
1 ATTN: R-P&VE-M, R. J. Schwinghamer  
1 SGE-ME-MM, Mr. W. A. Wilson, Building 4720

1 Ship Research Committee, Maritime Transportation Research Board, National  
Research Council, 2101 Constitution Ave., N. W., Washington, D. C. 20418

1 Materials Sciences Corporation, Blue Bell Campus, Marion Towle Building,  
Blue Bell, Pennsylvania 19422

Wyman-Gordon Company, Worcester, Massachusetts 01601  
1 ATTN: Technical Library

Lockheed-Georgia Company, Marietta, Georgia 30063  
1 ATTN: Advanced Composites Information Center, Dept. 72-54 - Zone 26

General Dynamics, Convair Aerospace Division, P.O. Box 748,  
Fort Worth, Texas 76101  
1 ATTN: Mfg. Engineering Technical Library

1 Mechanical Properties Data Center, Relfour Stulen Inc.,  
13917 W. Bay Shore Drive, Traverse City, Missouri 49684

Director, Army Materials and Mechanics Research Center,  
Watertown, Massachusetts 02172

2 ATTN: DRXMR-PL  
1 DRXMR-AP  
1 DRXMR-X  
1 DRXMR-XP  
1 DRXMR-E  
30 DRXMR-EM  
1 DRXMR-CT  
1 -Author



<p>Army Materials and Mechanics Research Center, Watertown, Massachusetts 02172 DEFORMATION OF TEXTURED STEELS - A. K. Ghosh and N. E. Paton, Rockwell International Science Center, Thousand Oaks, California 91360</p> <p>Final Report AMRC TR 78-40, September 1978. 45 pp - illus., Contract DAG-46-77-C-0054 D/A Project: IL162105ANB4, ANMS Code: 312105.HB40011, Final Report, August 15, 1977 to August 15, 1978.</p> <p>Key words: Texture Preferred Orientation Alloy Steel Deformation Ballistics Compression Tests</p> <p>The present research program was designed to investigate the influence of crystallographic texture on the mechanical strength of steel plates subjected to various loading conditions including ballistic impact. The steels of interest are 5% Ni martensitic steels containing varying intensities of (111) and (112) textures, thermomechanically processed by etching and rolling. The investigation includes calculations of theoretical strength for shear and through-thickness compression modes for the various ideal textures by computation of the appropriate Taylor factors. The experimental part of the program involved shear testing samples taken from various angles in the plates, as well as conducting through-thickness compression tests. Both the theoretical and experimental work indicate that the through-thickness compression resistance increases with increasing (111) and (112) texture intensity, and the compression resistance appears to be the dominant factor in controlling ballistic perforation resistance. An analysis of failure modes for plates of different ideal textures has also been made.</p>	<p>AD _____ UNCLASSIFIED UNLIMITED DISTRIBUTION</p>
<p>Army Materials and Mechanics Research Center, Watertown, Massachusetts 02172 DEFORMATION OF TEXTURED STEELS - A. K. Ghosh and N. E. Paton, Rockwell International Science Center, Thousand Oaks, California 91360</p> <p>Final Report AMRC TR 78-40, September 1978. 45 pp - illus., Contract DAG-46-77-C-0054 D/A Project: IL162105ANB4, ANMS Code: 312105.HB40011, Final Report, August 15, 1977 to August 15, 1978.</p> <p>Key words: Texture Preferred Orientation Alloy Steel Deformation Ballistics Compression Tests</p> <p>The present research program was designed to investigate the influence of crystallographic texture on the mechanical strength of steel plates subjected to various loading conditions including ballistic impact. The steels of interest are 5% Ni martensitic steels containing varying intensities of (111) and (112) textures, thermomechanically processed by etching and rolling. The investigation includes calculations of theoretical strength for shear and through-thickness compression modes for the various ideal textures by computation of the appropriate Taylor factors. The experimental part of the program involved shear testing samples taken from various angles in the plates, as well as conducting through-thickness compression tests. Both the theoretical and experimental work indicate that the through-thickness compression resistance increases with increasing (111) and (112) texture intensity, and the compression resistance appears to be the dominant factor in controlling ballistic perforation resistance. An analysis of failure modes for plates of different ideal textures has also been made.</p>	<p>AD _____ UNCLASSIFIED UNLIMITED DISTRIBUTION</p>
<p>Army Materials and Mechanics Research Center, Watertown, Massachusetts 02172 DEFORMATION OF TEXTURED STEELS - A. K. Ghosh and N. E. Paton, Rockwell International Science Center, Thousand Oaks, California 91360</p> <p>Final Report AMRC TR 78-40, September 1978. 45 pp - illus., Contract DAG-46-77-C-0054 D/A Project: IL162105ANB4, ANMS Code: 312105.HB40011, Final Report, August 15, 1977 to August 15, 1978.</p> <p>Key words: Texture Preferred Orientation Alloy Steel Deformation Ballistics Compression Tests</p> <p>The present research program was designed to investigate the influence of crystallographic texture on the mechanical strength of steel plates subjected to various loading conditions including ballistic impact. The steels of interest are 5% Ni martensitic steels containing varying intensities of (111) and (112) textures, thermomechanically processed by etching and rolling. The investigation includes calculations of theoretical strength for shear and through-thickness compression modes for the various ideal textures by computation of the appropriate Taylor factors. The experimental part of the program involved shear testing samples taken from various angles in the plates, as well as conducting through-thickness compression tests. Both the theoretical and experimental work indicate that the through-thickness compression resistance increases with increasing (111) and (112) texture intensity, and the compression resistance appears to be the dominant factor in controlling ballistic perforation resistance. An analysis of failure modes for plates of different ideal textures has also been made.</p>	<p>AD _____ UNCLASSIFIED UNLIMITED DISTRIBUTION</p>

The present research program was designed to investigate the influence of crystallographic texture on the mechanical strength of steel plates subjected to various loading conditions including ballistic impact. The steels investigated were of two different grades, A533-B and A508-2. The (111) and (112) textures, thermomechanically processed by Hu et al.<sup>11</sup> The investigation includes calculations of theoretical strength for shear and through-thickness compression modes for the various ideal textures by compilation of the appropriate Taylor factors. The experimental part of the program involved shear testing samples taken from various angles in the plates, as well as conducting through-thickness compression tests. Both theoretical and experimental work indicate that the through-thickness compression resistance increases with increasing (111) and (112) texture. The shear resistance appears to be insensitive to texture. An analysis of failure modes for plates of different ideal textures has also been made.

The present research program was designed to investigate the influence of the microcrystalllographic texture on the mechanical strength of steel plates subjected to various loading conditions including ballistic impact. The steels of interest are 55 Ni martensitic steels containing varying intensities of (111), (110) and (112) textures. Thermomechanically processed plates of 1000 MPa yield strength and 1.5 mm thickness were used for the investigation. The investigation includes the determination of the mechanical strength for shear and compression for the various ideal textures by comparison of the experimental results with the theoretical prediction based on the compression resistance model for the experimental part of the investigation. The compression resistance model for the experimental part of the investigation involved shear testing samples taken from various angles in the plates, as well as conducting through-thickness compression tests. Both the theoretical and experimental work indicate that the through-thickness compression resistance increases with increasing (111) and (112) texture intensity, and the compression resistance appears to be the dominant factor controlling ballistic performance resistance to the onset of failure. The compression resistance model was also been made.

The present research program was designed to investigate the influence of crystallographic texture on the mechanical strength of steel plates, subjected to various loading conditions including ballistic impact. The steels of interest are 5% Ni martensitic steels containing varying intensities of (111) and (112) textures, thermomechanically processed by Hu et al.<sup>1</sup> The investigation includes calculations of theoretical strength for shear and through-thickness compression modes for the various final textures by computation of the appropriate slip factors. The experiments were applied to the validation of the theoretical calculations and to the comparison with the results of compression tests, as well as conducting through-thickness compression tests. Both the theoretical and experimental work indicate that the through-thickness compression resistance increases with increasing (111) and (112) texture intensity, and the compression resistance appears to be the dominant factor in controlling ballistic performance resistance. An analysis of failure

The present research program was designed to investigate the influence of crystallographic texture on the mechanical strength of steel plates subjected to various loading conditions including ballistic impact. The steels of interest are 55 Ni maritensitic steels containing varying amounts of Mn, (111) and (112) textures, thermomechanically processed by Hu et al.<sup>11</sup> The program involves three basic compression modes for the various ideal textures by computation of the appropriate Taylor factors. The experimental part of the program involved shear testing samples taken from various angles in the plates, as well as conducting through-thickness compression tests. Both the theoretical and experimental work indicate that the through-thickness compression resistance increases with increasing (111) and (112) texture intensity, and the compression resistance appears to be the dominant factor in controlling ballistic performance resistance. This analysis is a preliminary study, and more detailed work is also planned.